Cancer Cell, Volume *39*

Supplemental information

Promotion of cholangiocarcinoma growth by diverse cancer-associated fibroblast subpopulations

Silvia Affo, Ajay Nair, Francesco Brundu, Aashreya Ravichandra, Sonakshi Bhattacharjee, Michitaka Matsuda, LiKang Chin, Aveline Filliol, Wen Wen, Xinhua Song, Aubrianna Decker, Jeremy Worley, Jorge Matias Caviglia, Lexing Yu, Deqi Yin, Yoshinobu Saito, Thomas Savage, Rebecca G. Wells, Matthias Mack, Lars Zender, Nicholas Arpaia, Helen E. Remotti, Raul Rabadan, Peter Sims, Anne-Laure Leblond, Achim Weber, Marc-Oliver Riener, Brent R. Stockwell, Jellert Gaublomme, Josep M. Llovet, Raghu Kalluri, George K. Michalopoulos, Ekihiro Seki, Daniela Sia, Xin Chen, Andrea Califano, and Robert F. Schwabe

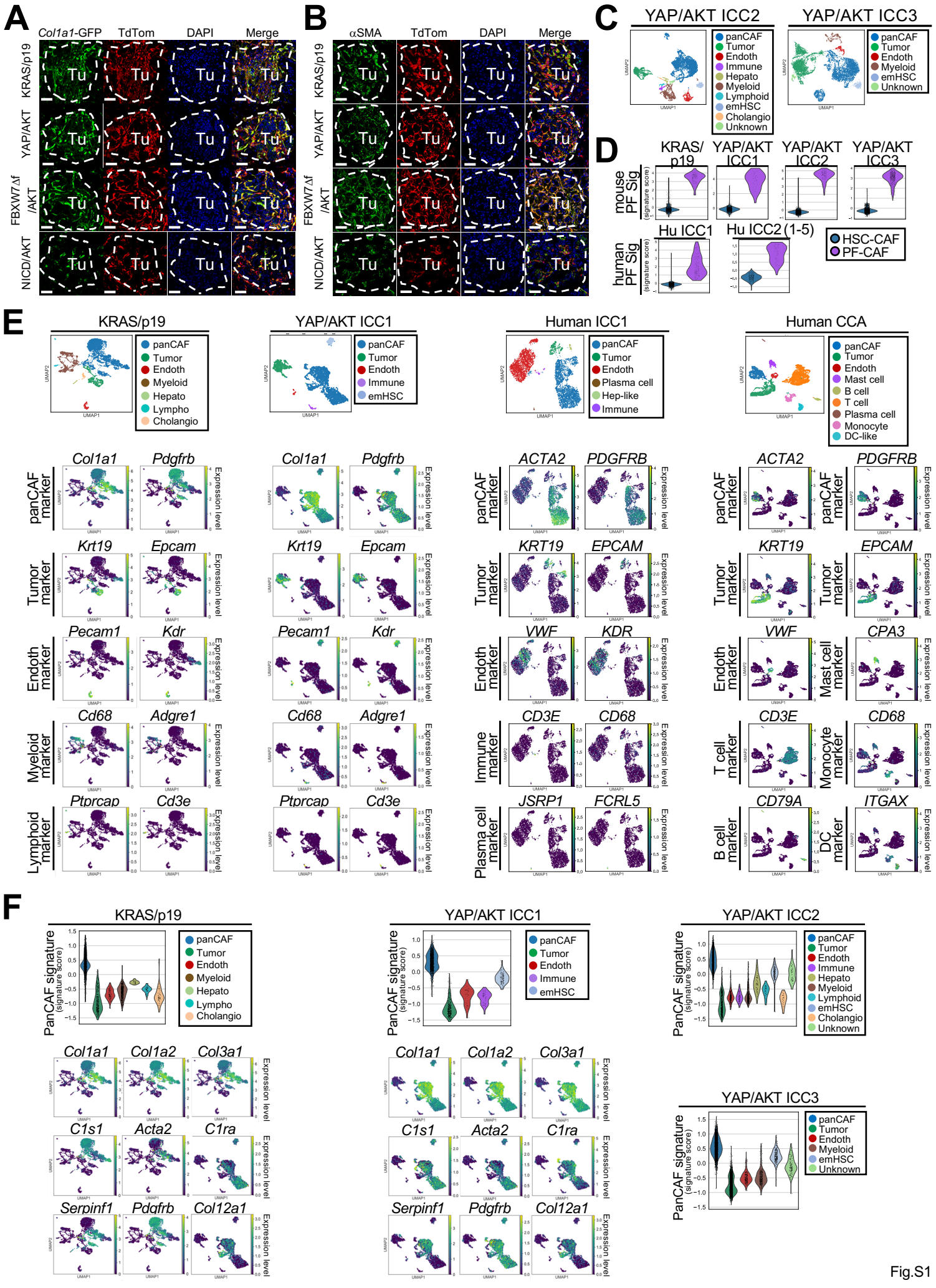
A
Col1a1-GFP
TdTom
DAPI
Merge
KRAS/p19
YAP/AKT
FBXW7Δf /AKT
NICD/AKT
Tu
B
αSMA
TdTom
DAPI
Merge
C
YAP/AKT ICC2
YAP/AKT ICC3
panCAF
Tumor
Endoth
Immune
Hepato
Myeloid
Lymphoid
emHSC
Cholangio
Unknown
D
KRAS/ p19
YAP/AKT ICC1
YAP/AKT ICC2
YAP/AKT ICC3
mouse PF Sig
(signature score)
Hu ICC1
Hu ICC2 (1-5)
human PF Sig
HSC-CAF
PF-CAF
E
KRAS/p19
YAP/AKT ICC1
Human ICC1
Human CCA
Lympho
Plasma cell
Hep-like
Mast cell
B cell
T cell
Monocyte
DC-like
panCAF marker
Tumor marker
Endoth marker
Myeloid marker
Lymphoid marker
Immune marker
Mast cell marker
T cell marker
Monocyte marker
B cell marker
DC marker
Col1a1
Pdgfrb
ACTA2
PDGFRB
Krt19
Epcam
KRT19
EPCAM
Pecam1
Kdr
VWF
KDR
CPA3
Cd68
Adgre1
CD3E
CD68
Ptprcap
Cd3e
JSRP1
FCRL5
CD79A
ITGAX
Expression level
UMAP1
UMAP2
F
PanCAF signature
(signature score)
Col1a2
Col3a1
C1s1
Acta2
C1ra
Serpinf1
Pdgfrb
Col12a1

Fig.S1

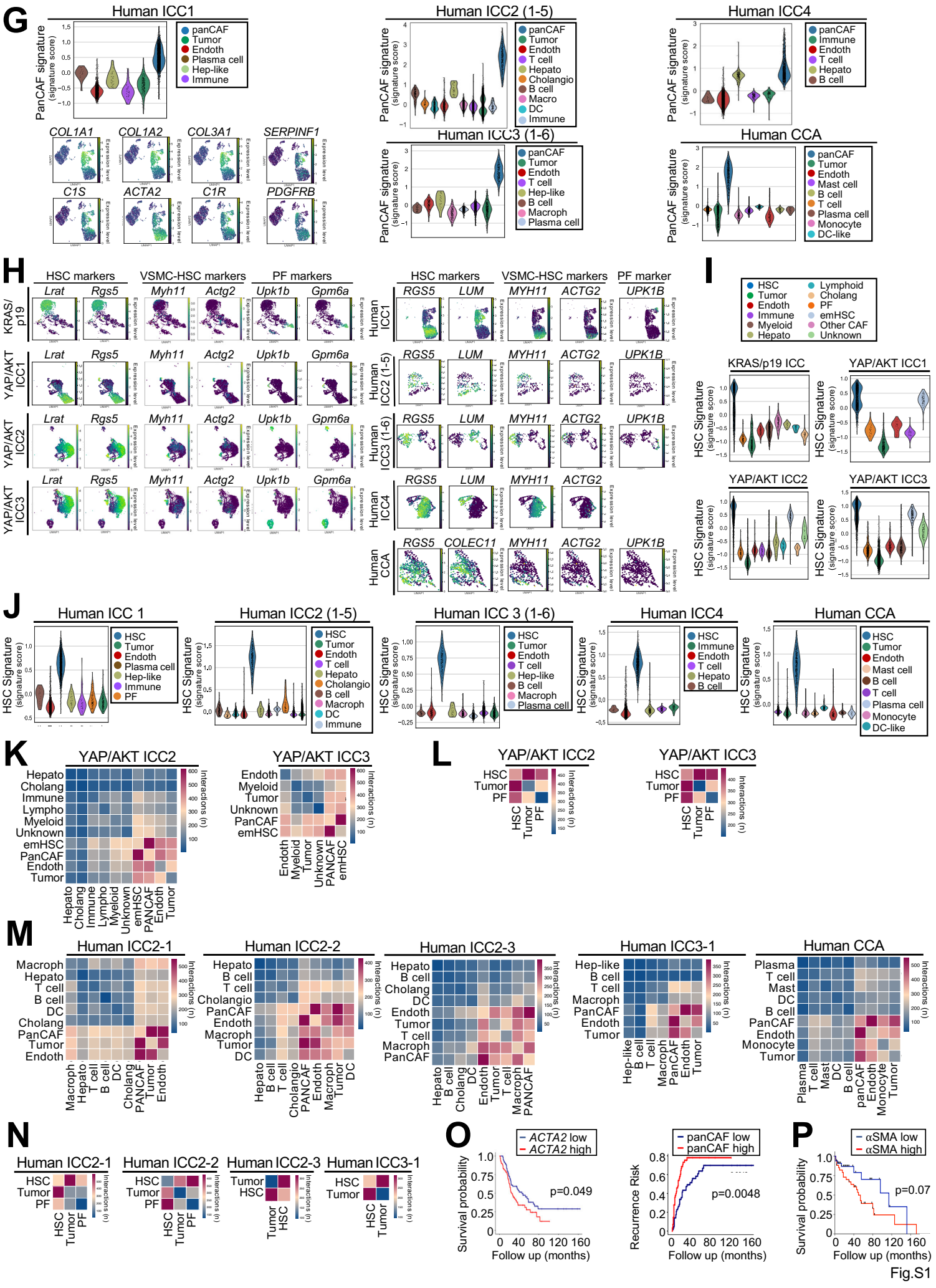
G
Human ICC1
Human ICC2 (1-5)
Human ICC4
Human ICC3 (1-6)
Human CCA
PanCAF signature (signature score)
panCAF
Tumor
Endoth
Plasma cell
Hep-like
Immune
T cell
Hepato
Cholangio
B cell
Macro
DC
Mast cell
Monocyte
DC-like
COL1A1
COL1A2
COL3A1
SERPINF1
C1S
ACTA2
C1R
PDGFRB
H
HSC markers
VSMC-HSC markers
PF markers
Lrat
Rgs5
Myh11
Actg2
Upk1b
Gpm6a
RGS5
LUM
MYH11
ACTG2
UPK1B
COLEC11
KRAS/ p19
YAP/AKT ICC1
YAP/AKT ICC2
YAP/AKT ICC3
Human ICC1
Human ICC2 (1-5)
Human ICC3 (1-6)
Human ICC4
Human CCA
I
HSC
Tumor
Endoth
Immune
Myeloid
Hepato
Lymphoid
Cholang
PF
emHSC
Other CAF
Unknown
KRAS/p19 ICC
YAP/AKT ICC1
YAP/AKT ICC2
YAP/AKT ICC3
HSC Signature (signature score)
J
Human ICC 1
Human ICC2 (1-5)
Human ICC 3 (1-6)
Human ICC4
Human CCA
K
YAP/AKT ICC2
YAP/AKT ICC3
Interactions (n)
Hepato
Cholang
Immune
Lympho
Myeloid
Unknown
emHSC
PanCAF
Endoth
Tumor
L
M
Human ICC2-1
Human ICC2-2
Human ICC2-3
Human ICC3-1
Human CCA
N
Human ICC2-1
Human ICC2-2
Human ICC2-3
Human ICC3-1
O
ACTA2 low
ACTA2 high
p=0.049
Survival probability
Follow up (months)
panCAF low
panCAF high
p=0.0048
Recurrence Risk
P
αSMA low
αSMA high
p=0.07

Fig.S1

Figure S1 (Related to Figure 1) | CAF origin and interactions with tumor cells in murine and human ICC. (A,B) Representative images of confocal microscopy showing co-localization of *Lrat*-Cre-induced TdTom with CAF markers *Col1a1*-GFP (A) or αSMA (B) in KRAS/p19-, YAP/AKT-, FBXW7ΔF/AKT-, NICD/AKT-induced ICC (n=3 per model) in *Lrat*-Cre^{+} TdTom^{+} *Col1a1*-GFP^{+} mice. Scale bars, 50 μm. (C) UMAPs of scRNA-seq showing all detected cell populations in the indicated samples. (D) Violin plots of scRNA-seq showing the PF signature score in the indicated samples; the width of each violin plot indicates the kernel density of the expression values. (E) UMAPs of scRNA-seq showing all detected cell populations and the normalized expression levels of indicated genes. (F,G) Violin plots showing the panCAF signature score in the indicated samples and UMAPs showing the normalized expression levels of indicated genes in (F) mouse ICC models (n=4) and in (G) human ICC (n=4) and human CCA (n=1). (H) UMAPs of scRNA-seq showing the normalized expression levels of HSC-CAF, VSMC-HSC and PF-CAF markers within panCAF in the indicated samples. (I,J) Violin plots of scRNA-seq showing the HSC signature score in (I) mouse ICC (n=4) and in (J) human ICC (n=4) and human CCA (n=1); the width of each violin plot indicates the kernel density of the expression values. (K-N) Heatmaps of scRNA-seq showing number of ligand-receptor interactions between (K,M) all cell populations and between (L,N) HSC-CAF, PF-CAF and tumor cells detected by CellphoneDB in the indicated YAP/AKT-induced ICC (n=2), human ICC (n=4) and human CCA (n=1). (O) Overall survival in 119 ICC patients with low (n=59) and high (n=60) *ACTA2* mRNA expression and recurrence risk in 113 ICC patients with low (n=56) and high (n=57) panCAF signature (Sia et al. cohort). (P) Overall survival in CCA patients with low (n=37) or high (n=40) expression of αSMA (Riener et al. TMA cohort).

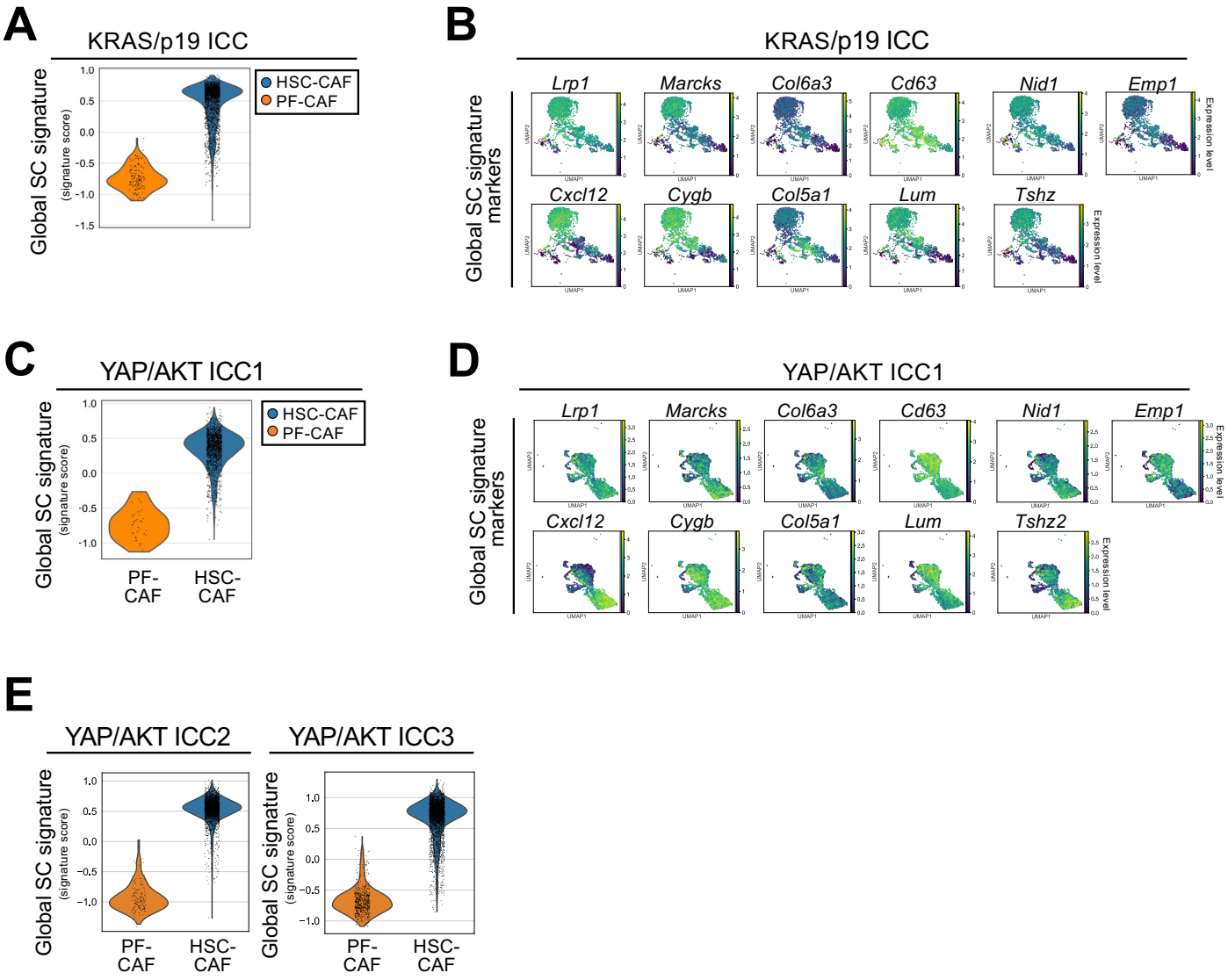
A
KRAS/p19 ICC
Global SC signature
(signature score)
HSC-CAF
PF-CAF
B
KRAS/p19 ICC
Global SC signature markers
Lrp1
Marcks
Col6a3
Cd63
Nid1
Emp1
Cxcl12
Cygb
Col5a1
Lum
Tshz
Expression level
C
YAP/AKT ICC1
PF-CAF
HSC-CAF
D
YAP/AKT ICC1
Tshz2
E
YAP/AKT ICC2
YAP/AKT ICC3

Fig.S2

Figure S2 (Related to Figure 2) | Comparison of CAF from ICC and PDAC by global stellate cell and portal fibroblast signatures by single cell RNA-sequencing. (A) Violin plot showing the global SC signature in KRAS/p19-induced ICC (n=1). The width of each violin plot indicates the kernel density of the expression values. (B) UMAPs showing the normalized expression levels of the global stellate cell (global SC) signature markers in KRAS/p19 ICC. (C,E) Violin plot showing the global SC signature relative to randomly selected genes in YAP/AKT-induced ICC (n=3). The width of each violin plot indicates the kernel density of the expression values. (D) UMAPs showing the normalized expression levels of the global stellate cell (global SC) signature markers in YAP/AKT ICC (n=1).

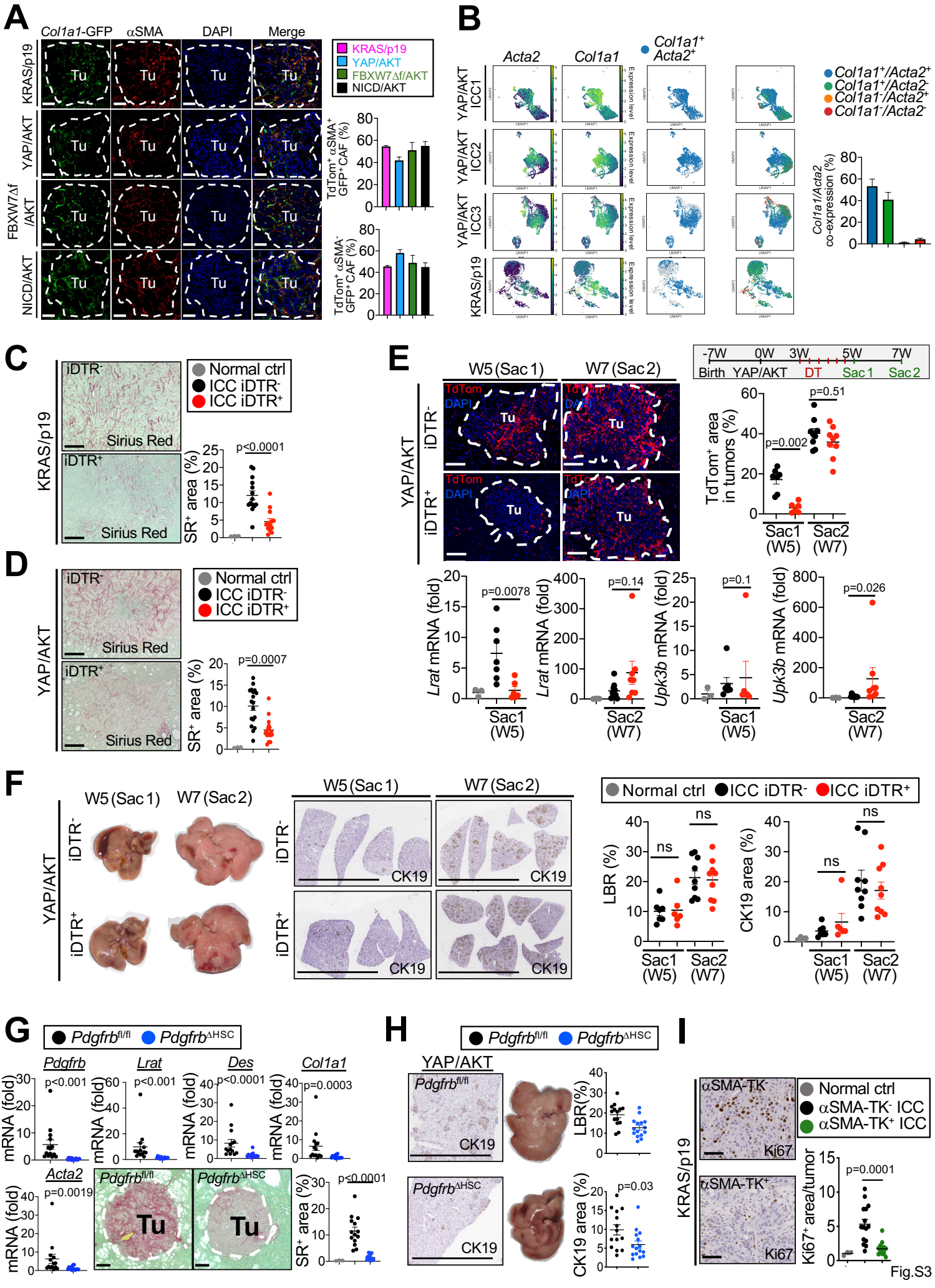
A
Col1a1-GFP
αSMA
DAPI
Merge
KRAS/p19
YAP/AKT
FBXW7Δf/AKT
NICD/AKT
Tu
KRAS/p19
YAP/AKT
FBXW7Δf/AKT
NICD/AKT
TdTom+ αSMA+ GFP+CAF (%)
TdTom+ αSMA- GFP+CAF (%)
B
Acta2
Col1a1
Col1a1+ Acta2+
YAP/AKT ICC1
YAP/AKT ICC2
YAP/AKT ICC3
KRAS/p19
Col1a1+/Acta2+
Col1a1+/Acta2-
Col1a1-/Acta2+
Col1a1-/Acta2-
Col1a1/Acta2 co-expression (%)
C
iDTR-
iDTR+
Sirius Red
Normal ctrl
ICC iDTR-
ICC iDTR+
SR+ area (%)
p<0.0001
D
YAP/AKT
p=0.0007
E
W5 (Sac 1)
W7 (Sac 2)
TdTom
DAPI
Tu
-7W
0W
3W
5W
7W
Birth
YAP/AKT
DT
Sac 1
Sac 2
TdTom+ area in tumors (%)
p=0.002
p=0.51
Sac1 (W5)
Sac2 (W7)
Lrat mRNA (fold)
p=0.0078
p=0.14
Upk3b mRNA (fold)
p=0.1
p=0.026
F
CK19
LBR (%)
CK19 area (%)
ns
G
Pdgfrb fl/fl
Pdgfrb ΔHSC
Pdgfrb
Lrat
Des
Col1a1
Acta2
mRNA (fold)
p<0.001
p<0.0001
p=0.0003
p=0.0019
SR+ area (%)
H
YAP/AKT
LBR(%)
CK19 area (%)
p=0.03
I
αSMA-TK-
αSMA-TK+
Normal ctrl
αSMA-TK- ICC
αSMA-TK+ ICC
Ki67
KRAS/p19
Ki67+ area/tumor
p=0.0001

Fig.S3

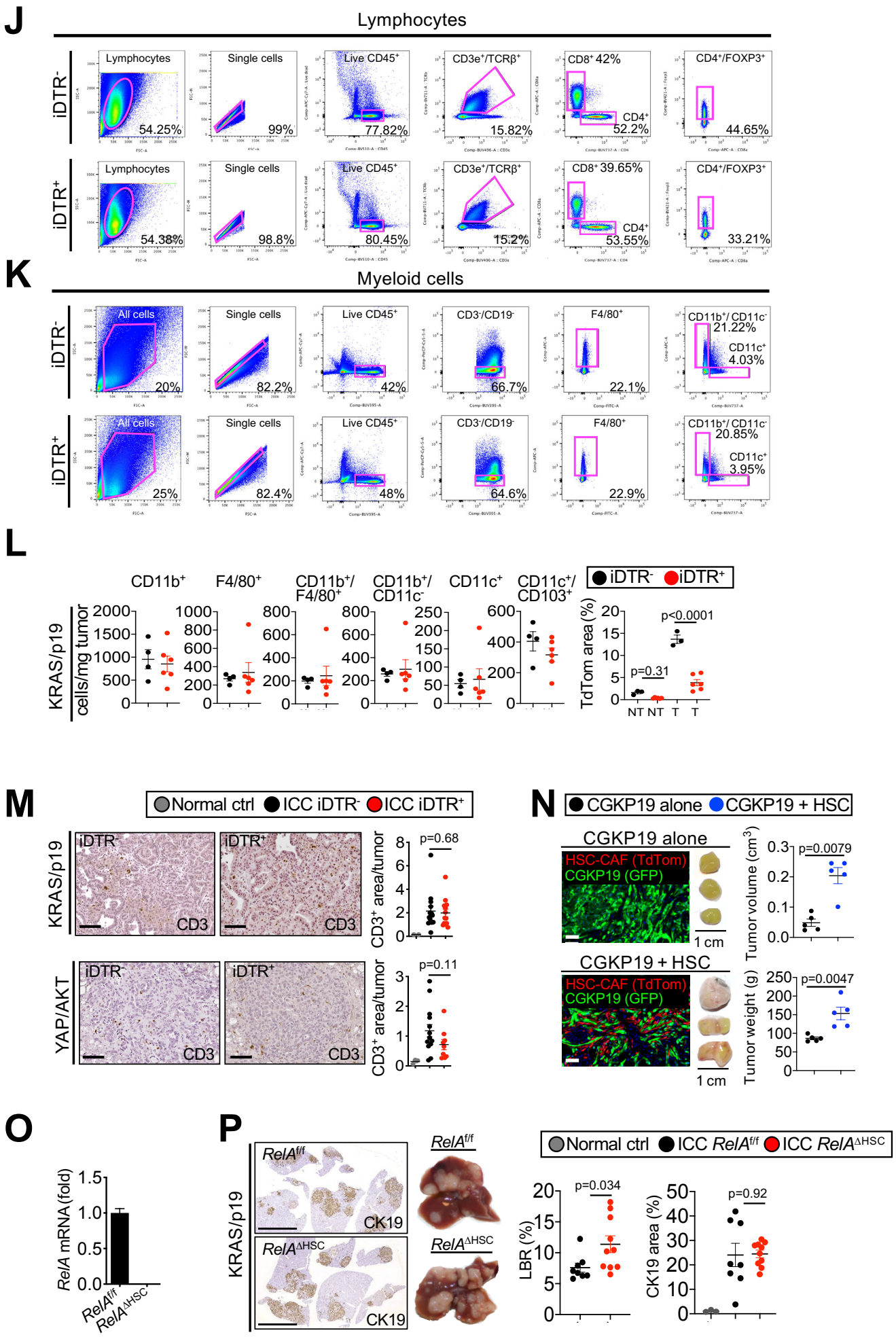
J
Lymphocytes
iDTR-
iDTR+
Lymphocytes
Single cells
Live CD45+
CD3e+/TCRβ+
CD8+ 42%
CD4+
CD4+/FOXP3+
54.25%
99%
77.82%
15.82%
52.2%
44.65%
54.38%
98.8%
80.45%
15.2%
CD8+ 39.65%
53.55%
33.21%
K
Myeloid cells
All cells
CD3-/CD19-
F4/80+
CD11b+/ CD11c-
CD11c+
20%
82.2%
42%
66.7%
22.1%
21.22%
4.03%
25%
82.4%
48%
64.6%
22.9%
20.85%
3.95%
L
CD11b+
F4/80+
CD11b+/ F4/80+
CD11b+/ CD11c-
CD11c+
CD11c+/ CD103+
iDTR- iDTR+
KRAS/p19 cells/mg tumor
TdTom area (%)
p<0.0001
p=0.31
NT NT T T
M
Normal ctrl ICC iDTR- ICC iDTR+
KRAS/p19
YAP/AKT
iDTR-
iDTR+
CD3
CD3+ area/tumor
p=0.68
p=0.11
N
CGKP19 alone CGKP19 + HSC
CGKP19 alone
CGKP19 + HSC
HSC-CAF (TdTom)
CGKP19 (GFP)
1 cm
Tumor volume (cm3)
Tumor weight (g)
p=0.0079
p=0.0047
O
RelA mRNA (fold)
RelAf/f
RelAΔHSC
P
KRAS/p19
RelAf/f
RelAΔHSC
CK19
Normal ctrl ICC RelAf/f ICC RelAΔHSC
LBR (%)
CK19 area (%)
p=0.034
p=0.92

Fig.S3

Figure S3 (Related to Figure 3) | CAF promote ICC. (A) Representative images of confocal microscopy and quantifications showing co-localization of *Col1a1*-GFP and αSMA in KRAS/p19-, YAP/AKT-, FBXW7ΔF/AKT-, NICD/AKT-induced ICC (n=3 per model) in *Lrat*-Cre^{+} TdTom^{+} *Col1a1*-GFP^{+} mice. Scale bars, 50 μm. (B) UMAPs of scRNA-seq showing the normalized expression levels of indicated genes and populations and quantifications of *Col1a1* and *Acta2* in KRAS/p19- (n=1) and YAP/AKT-induced ICC (n=3). (C,D) HSC-derived CAF were depleted by injecting diphtheria toxin 6 times (3x/week) in *Lrat*-Cre^{+}, TdTom^{+}, iDTR^{+} or *Lrat*-Cre^{+}, TdTom^{+}, iDTR^{-} littermates from week 5 to 7 after tumor induction (late depletion) and HSC depletion was confirmed by sirius red staining in (C) KRAS/p19 (n=13-15 mice/group) and (D) YAP/AKT-induced ICC (n=11-16 iDTR- mice/group). Scale bar 100 μm. (E-F) For early HSC-derived CAF depletion, *Lrat*-Cre^{+} TdTom^{+} iDTR^{+} mice and *Lrat*-Cre^{+} TdTom^{+} iDTR^{-} littermate controls were injected 6 times with DT (3x/week) starting 3 weeks after the plasmid injection. (E) HSC-derived CAF depletion and repopulation by HSC-CAF or PF-CAF were determined by measuring the TdTom^{+} area and *Lrat* (HSC marker) as well as *Upk3b* (PF marker) mRNA expression in YAP/AKT-induced ICC after the last DT injection (sac1, n=6-7 mice per group) or 2 weeks later (sac2, n=9 mice per group); (F) representative images of whole livers, liver body ratio (LBR), IHC and CK19^{+} quantifications from above groups. Scale bars 1 cm. (G-H) *Pdgfrb*, *Lrat*, *Des*, *Col1a1*, *Acta2* mRNA expression and representative images of sirius red and quantifications in *Pdgfrβ*$^{f/f}$ (n=14) and *Pdgfrβ*$^{\Delta HSC}$ (n=15) mice in YAP/AKT-induced ICC (G). Scale bar 100 μm. Representative images of livers, CK19 IHC as well as quantification of LBR and CK19^{+} area from above groups (H). Scale bars 1 cm. (I) Representative micrographs and quantifications of Ki67 IHC from KRAS/p19-induced ICC in αSMA-TK mice (n=15 mice/group). Scale bars 100 μm. (J,K) Representative gating strategy in the tumors of KRAS/p19-induced ICC, iDTR^{-} (n=4) and iDTR^{+} (n=6) mice for (J) lymphoid and (K) myeloid subsets. (L) Flow cytometric analysis of CD11b^{+}, F4/80^{+}, CD11b^{+}/F4/80^{+}, CD11b^{+}/CD11c^{-}, CD11c^{+}, CD11c^{+}/CD103^{+} subsets in the tumors from KRAS/p19-induced ICC as well as confirmation of depletion via TdTom^{+} area in *Lrat*-Cre^{+}TdTom^{+} iDTR^{-} (n=4) and *Lrat*-Cre^{+}TdTom^{+} iDTR^{+} (n=6) mice. (M) Representative micrographs and quantifications of CD3 IHC from KRAS/p19-induced ICC (n=14 iDTR^{-} mice, n=13 iDTR^{+} mice) and YAP/AKT-induced ICC (n=14 iDTR^{-} mice, n=9 iDTR^{+} mice). Scale bars 100 μm. (N) Subcutaneous co-injections of CGKP19 KRAS/p19 ICC-derived cells alone or with HSC in *Rag2*KO mice. (O) *RelA* mRNA expression in HSC from *RelA*$^{f/f}$ (n=2) and *RelA*$^{\Delta HSC}$ (n=2). (P) Representative images of CK19 IHC, livers, LBR and CK19^{+} area from RelA$^{f/f}$ (n=8) and RelA$^{\Delta HSC}$ (n=10) from KRAS/p19-induced ICC. For panels A-I, L-P data are shown as mean ± SEM, and statistical significance was determined using two-sided unpaired T-test (G,H,L,N) or Mann-Whitney (F,H,L,N,P) for groups of two; and by one-way ANOVA followed by Sidak's posthoc test (C,E,F,M,P) or Kruskal-Wallis test with Dunn's posthoc test (A,B,D,G,I) for groups of three.

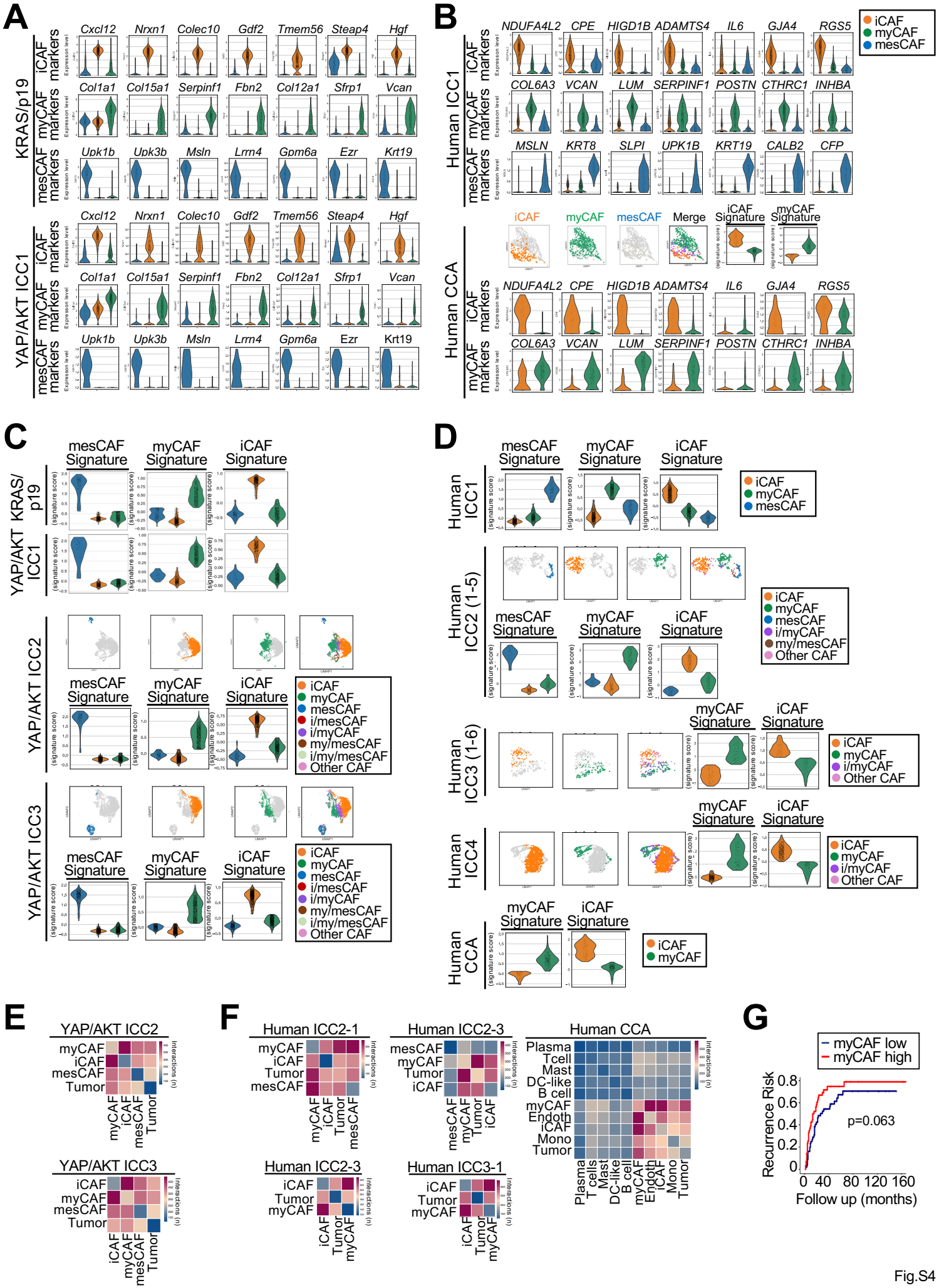
A
KRAS/p19
YAP/AKT ICC1
iCAF markers
myCAF markers
mesCAF markers
Cxcl12
Nrxn1
Colec10
Gdf2
Tmem56
Steap4
Hgf
Col1a1
Col15a1
Serpinf1
Fbn2
Col12a1
Sfrp1
Vcan
Upk1b
Upk3b
Msln
Lrrn4
Gpm6a
Ezr
Krt19
B
Human ICC1
Human CCA
NDUFA4L2
CPE
HIGD1B
ADAMTS4
IL6
GJA4
RGS5
COL6A3
VCAN
LUM
SERPINF1
POSTN
CTHRC1
INHBA
MSLN
KRT8
SLPI
UPK1B
KRT19
CALB2
CFP
iCAF
myCAF
mesCAF
Merge
iCAF Signature
myCAF Signature
C
YAP/AKT ICC2
YAP/AKT ICC3
mesCAF Signature
myCAF Signature
iCAF Signature
(signature score)
i/mesCAF
i/myCAF
my/mesCAF
i/my/mesCAF
Other CAF
D
Human ICC1
Human ICC2 (1-5)
Human ICC3 (1-6)
Human ICC4
Human CCA
E
YAP/AKT ICC2
YAP/AKT ICC3
Interactions (n)
F
Human ICC2-1
Human ICC2-3
Human CCA
Human ICC2-3
Human ICC3-1
Plasma
Tcell
Mast
DC-like
B cell
Endoth
Mono
Tumor
G
myCAF low
myCAF high
Recurrence Risk
p=0.063
Follow up (months)

Fig.S4

Figure S4 (Related to Figure 4) | Single cell RNA-sequencing of CAF subpopulations in murine and human ICC. (A,B) Violin plots showing the normalized expression levels of the top genes from iCAF, myCAF and mesCAF signatures in (A) KRAS/p19- , YAP/AKT-induced ICC and (B) human ICC and CCA in one representative sample each. (C,D) Violin plots showing the iCAF, myCAF and mesCAF signature scores in the indicated (C) KRAS/p19- induced ICC, YAP/AKT-induced ICC, (D) human ICC and human CCA samples. The width of each violin plot indicates the kernel density of the expression values. (E,F) Heatmaps showing number of ligand–receptor interactions between iCAF, myCAF, mesCAF and tumor cells in the indicated (E) YAP/AKT-induced ICC, (F) human ICC and human CCA samples, analyzed by CellPhone DB. (G) Recurrence risk in 113 ICC patients with low (n=56) and high (n=57) myCAF signature (Sia et al. cohort).

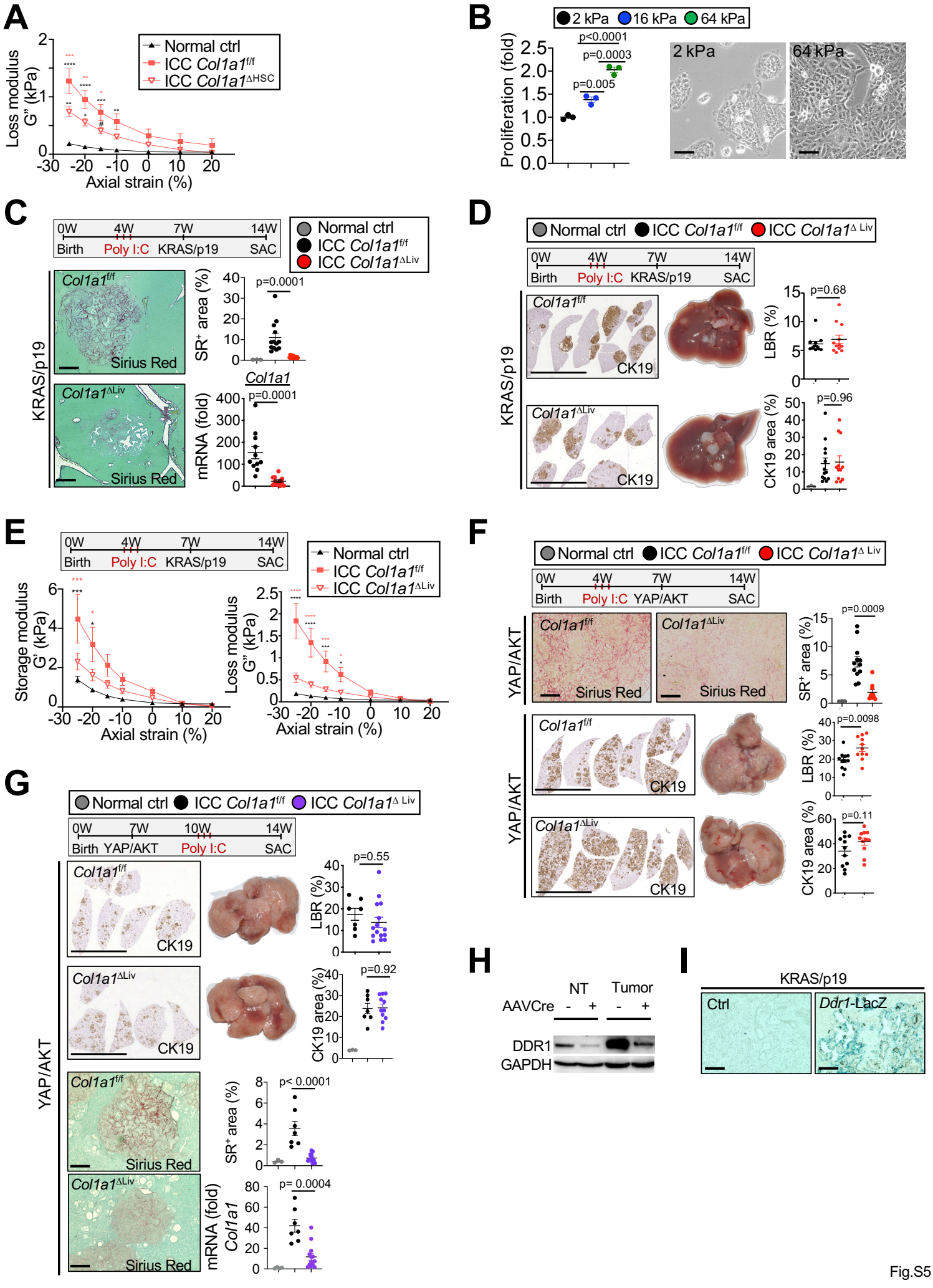
A
Loss modulus G'' (kPa)
Axial strain (%)
Normal ctrl
ICC Col1a1f/f
ICC Col1a1ΔHSC
B
2 kPa
16 kPa
64 kPa
Proliferation (fold)
p<0.0001
p=0.0003
p=0.005
2 kPa
64 kPa
C
0W 4W 7W 14W
Birth Poly I:C KRAS/p19 SAC
Normal ctrl
ICC Col1a1f/f
ICC Col1a1ΔLiv
KRAS/p19
Col1a1f/f
Col1a1ΔLiv
Sirius Red
SR+ area (%)
p=0.0001
Col1a1
mRNA (fold)
p=0.0001
D
Normal ctrl
ICC Col1a1f/f
ICC Col1a1Δ Liv
0W 4W 7W 14W
Birth Poly I:C KRAS/p19 SAC
KRAS/p19
CK19
LBR (%)
p=0.68
CK19 area (%)
p=0.96
E
0W 4W 7W 14W
Birth Poly I:C KRAS/p19 SAC
Normal ctrl
ICC Col1a1f/f
ICC Col1a1ΔLiv
Storage modulus G' (kPa)
Loss modulus G'' (kPa)
Axial strain (%)
F
Normal ctrl
ICC Col1a1f/f
ICC Col1a1Δ Liv
0W 4W 7W 14W
Birth Poly I:C YAP/AKT SAC
YAP/AKT
Col1a1f/f
Col1a1ΔLiv
Sirius Red
CK19
SR+ area (%)
p=0.0009
LBR (%)
p=0.0098
CK19 area (%)
p=0.11
G
Normal ctrl
ICC Col1a1f/f
ICC Col1a1Δ Liv
0W 7W 10W 14W
Birth YAP/AKT Poly I:C SAC
YAP/AKT
Col1a1f/f
Col1a1ΔLiv
CK19
Sirius Red
LBR (%)
p=0.55
CK19 area (%)
p=0.92
SR+ area (%)
p< 0.0001
mRNA (fold) Col1a1
p= 0.0004
H
NT
Tumor
AAVCre - + - +
DDR1
GAPDH
I
KRAS/p19
Ctrl
Ddr1-LacZ

Fig.S5

Figure S5 (Related to Figure 5) | CAF promote tumor growth independently of type I collagen. (A) Loss modulus G" (a measure of viscosity), was determined for tumors from *Col1a1*$^{f/f}$ (n=3) and *Col1a1*$^{\Delta HSC}$ (n=4) in a KRAS/p19-induced ICC and in control livers (n=2) by shear rheometry. Curves are mean ± SEM. Using 2-way ANOVA: *p≤0.05, **p≤0.01, ****p≤0.0001, #0.05<p≤0.10 vs ctrl (black) or vs *Col1a1*$^{\Delta HSC}$ (red). (B) Proliferation assessed by PicoGreen in HuCCT-1 plated on 2kPa, 16 kPa and 64 kPa plates (n=3 each group) and representative pictures of HuCCT-1 plated on 2kPa and 64 kPa plates. (C-E) Mx1-Cre activation for the deletion of *Col1a1* was induced by 3 i.p. injections of poly(I:C) before tumor induction starting when mice were 4 weeks old. (C) Representative images and quantification of sirius red staining and tumor *Col1a1* mRNA expression in *Col1a1*$^{f/f}$ (n=13) and *Col1a1*$^{\Delta Liv}$ (n=12) in KRAS/p19-induced ICC. Scale bars 100 μm. (D) Representative images of CK19 IHC, livers, LBR and CK19^{+} area from KRAS/p19-induced ICC for *Col1a1*$^{f/f}$ (n= 13) and *Col1a1*$^{\Delta Liv}$ (n=12) mice. Scale bars 1 cm. (E) Storage modulus G' (a measure of elasticity) and loss modulus G" (a measure of viscosity), were determined for tumors from *Col1a1*$^{f/f}$ (n=3) and *Col1a1*$^{\Delta Liv}$ (n=6) in KRAS/p19 ICC or control liver (n=2) by shear rheometry. Curves are mean ± SEM. Using 2-way ANOVA: *p≤0.05, **p≤0.01, ****p≤0.0001, #0.05<p≤0.10 vs ctrl (black) or vs *Col1a1*$^{\Delta Liv}$ (red). (F) Representative images and quantifications of sirius red staining, livers, LBR and the CK19^{+} area in *Col1a1*$^{f/f}$ (n=11) and *Col1a1*$^{\Delta Liv}$ (n=11) mice from YAP/AKT-induced ICC. Scale bars 1 cm**.** (G) *Mx1*-Cre activation for the deletion of *Col1a1* was induced by 3 i.p. injections of poly(I:C) starting 3 weeks after tumor induction. Representative images of sirius red staining and livers, LBR, *Col1a1* mRNA expression and the CK19 and sirius red-positive area in *Col1a1*$^{f/f}$ (n=7) and *Col1a1*$^{\Delta Liv}$ (n=11) mice from YAP/AKT-induced ICC. Scale bars 1 cm. (H) DDR1 western blot in *Ddr1*$^{f/f}$ NT (n=1) and T (n=1) and (I) representative XGAL staining in *Ddr1*-LacZ reporter (n=1) and wt littermate (n=1) mice in KRAS/p19-induced ICC. Data are shown as mean ± SEM, and statistical significance was determined by two-sided unpaired T-test (D,F) or Mann-Whitney (E) for groups of two; and by 2-way ANOVA (A,E) or one-way ANOVA (B,G) or Kruskal-Wallis test with Dunn's posthoc test (C,D) for groups of three.

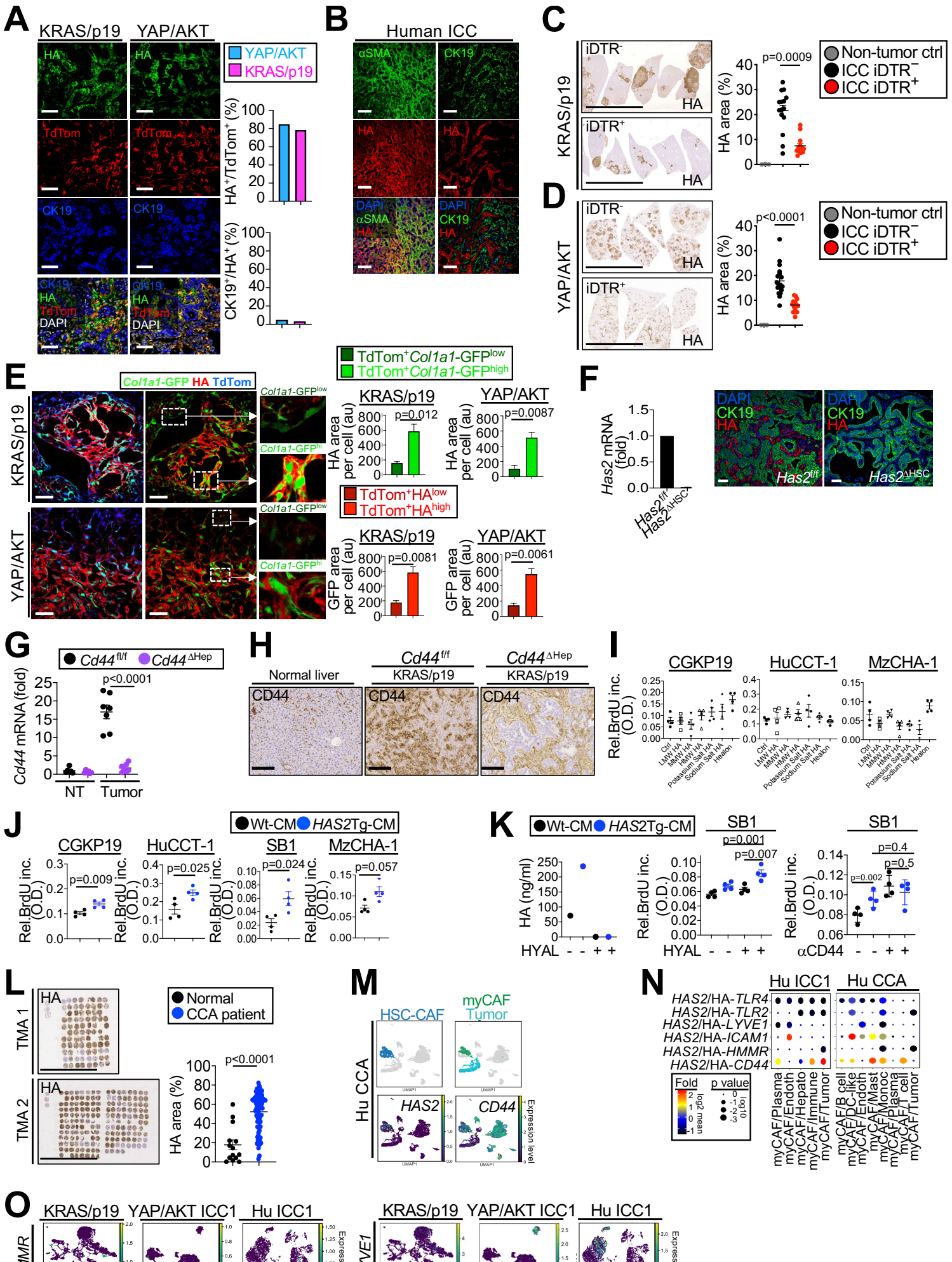
A
KRAS/p19
YAP/AKT
HA
TdTom
CK19
DAPI
YAP/AKT
KRAS/p19
HA+/TdTom+ (%)
CK19+/HA+ (%)
B
Human ICC
αSMA
CK19
HA
DAPI
C
KRAS/p19
iDTR-
iDTR+
HA area (%)
p=0.0009
Non-tumor ctrl
ICC iDTR-
ICC iDTR+
D
YAP/AKT
p<0.0001
E
Col1a1-GFP HA TdTom
TdTom+Col1a1-GFPlow
TdTom+Col1a1-GFPhigh
Col1a1-GFPlow
Col1a1-GFPhi
KRAS/p19
YAP/AKT
HA area per cell (au)
p=0.012
p=0.0087
TdTom+HAlow
TdTom+HAhigh
GFP area per cell (au)
p=0.0081
p=0.0061
F
Has2 mRNA (fold)
Has2f/f
Has2ΔHSC
DAPI
CK19
HA
G
Cd44f/f
Cd44ΔHep
Cd44 mRNA (fold)
p<0.0001
NT
Tumor
H
Normal liver
Cd44f/f
KRAS/p19
Cd44ΔHep
CD44
I
CGKP19
HuCCT-1
MzCHA-1
Rel.BrdU inc. (O.D.)
Ctrl
LMW HA
MMW HA
HMW HA
Potassium Salt HA
Sodium Salt HA
Healon
J
Wt-CM
HAS2Tg-CM
p=0.009
p=0.025
p=0.024
p=0.057
K
HA (ng/ml)
HYAL
SB1
p=0.001
p=0.007
αCD44
p=0.4
p=0.5
p=0.002
L
TMA 1
TMA 2
Normal
CCA patient
p<0.0001
M
HSC-CAF
myCAF Tumor
Hu CCA
HAS2
CD44
Expression level
N
Hu ICC1
Hu CCA
HAS2/HA-TLR4
HAS2/HA-TLR2
HAS2/HA-LYVE1
HAS2/HA-ICAM1
HAS2/HA-HMMR
HAS2/HA-CD44
Fold
p value
myCAF/Plasma
myCAF/Endoth
myCAF/Hepato
myCAF/Immune
myCAF/Tumor
myCAF/B cell
myCAF/DC-like
myCAF/Endoth
myCAF/Mast
myCAF/Monoc
myCAF/Plasma
myCAF/T cell
myCAF/Tumor
O
HMMR
LYVE1
KRAS/p19
YAP/AKT ICC1
Hu ICC1
UMAP1
Expression level

Fig.S6

Figure S6 (Related to Figure 6) | myCAF-derived HAS2 sustain tumor growth in ICC. (A) Representative micrograph and quantifications of confocal microscopy show co-localization of *Lrat*-Cre-induced TdTom (HSC derived-CAF) with HA and absent co-localization with CK19 in KRAS/p19- (n=1) and YAP/AKT- (n=1) ICC. (B) Confocal microscopy in human ICC (n=1) showed co-localization of HA with αSMA but not with CK19. Scale bars, 50 μm. (C,D) Representative micrographs of HA IHC and quantification in CAF-depleted mice from (C) KRAS/p19-ICC (n=15 $iDTR^-$, n=13 $iDTR^+$ mice) and (D) YAP/AKT-induced ICC (n=16 $iDTR^-$, n=11, $iDTR^+$ mice). Scale bars 1 cm. (E) Representative micrograph and quantifications of confocal microscopy show high expression of myCAF HA in cells with high expression of myCAF marker *Col1a1*-GFP and low expression of myCAF HA in cells with low expression of myCAF marker *Col1a1*-GFP, in KRAS/p19- and YAP/AKT-induced ICC (n=3 tumors per group). Scale bars, 50 μm. (F) *Has2* mRNA expression in HSC isolated from $Has2^{f/f}$ (n=1) and $Has2^{\Delta HSC}$ (n=2) and representative confocal microscopy showing absent HA in $Has2^{\Delta HSC}$ mice. Scale bars, 50 μm. (G) *Cd44* mRNA expression in tumor (T) (n=6 per group) and non-tumor (NT) (n=7 per group) tissue from $Cd44^{f/f}$ and $Cd44^{\Delta Hep}$ mice. (H) Representative micrographs of CD44 IHC in normal liver and tumor area in KRAS/p19-induced ICC in $Cd44^{f/f}$ and $Cd44^{\Delta Hep}$ mice. (I) BrdU incorporation assay in mouse (CGKP19) and human (HuCCT1 and MzCHA) tumor cells treated with different types of HA. (J) BrdU incorporation assay in human and mouse tumor cells treated with conditioned medium (CM) from *HAS2*-Tg and littermate wt mice (n=4/group). (K) HA content in the CM from *HAS2*-Tg and littermate control wt mice by ELISA in presence or absence of hyaluronidase (HYAL) (n=1 per condition, left panel) and BrdU incorporation assay in SB1 cells treated with CM from *HAS2*-Tg or littermate wt mice in the presence or absence of HYAL or after pre-treatment with CD44 antibody or IgG control (n=4 per condition, middle and right panel). (L) Representative micrographs and quantifications of HA-stained area of human CCA TMAs (n=19 ICC and n=58 ECC) and normal liver (n=14). Scale bars 1 cm. (M) UMAPs showing the normalized expression levels of *HAS2* and *CD44* in human CCA (n=1). (N) Representative CellphoneDB heatmap showing interactions of *HAS2*-expressing myCAF with HA-receptor expressing cells in human ICC and in CCA. (O) UMAPs showing the normalized expression levels of *HMMR* and *LYVE1* in KRAS/p19-, YAP/AKT-induced ICC and in human ICC. For panels C-E,G,I-L; data are shown as mean ± SEM, statistical significance was determined by two-sided unpaired T-test (J) or Mann-Whitney (J,L) groups of two; and by one-way ANOVA followed by Sidak's posthoc test (D,E,K,G,I) or Kruskal-Wallis test with Dunn's posthoc test (C,I) groups of three.

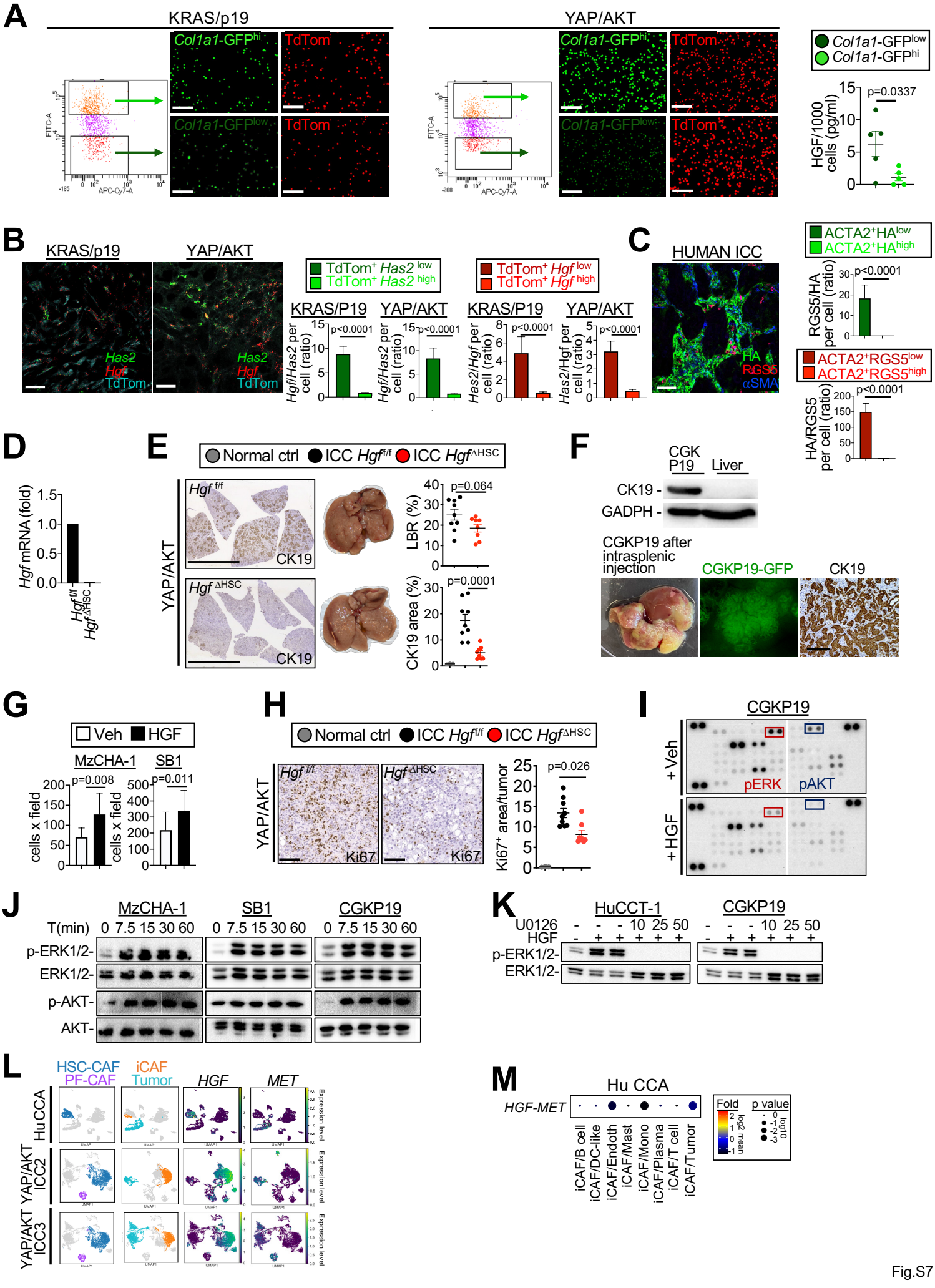
A
KRAS/p19
YAP/AKT
Col1a1-GFPhi
Col1a1-GFPlow
TdTom
FITC-A
APC-Cy7-A
Col1a1-GFPlow
Col1a1-GFPhi
HGF/1000 cells (pg/ml)
p=0.0337
B
KRAS/p19
YAP/AKT
Has2
Hgf
TdTom
TdTom+ Has2 low
TdTom+ Has2 high
TdTom+ Hgf low
TdTom+ Hgf high
Hgf/Has2 per cell (ratio)
Has2/Hgf per cell (ratio)
p<0.0001
C
HUMAN ICC
HA
RGS5
αSMA
ACTA2+HAlow
ACTA2+HAhigh
RGS5/HA per cell (ratio)
ACTA2+RGS5low
ACTA2+RGS5high
HA/RGS5 per cell (ratio)
D
Hgf mRNA (fold)
Hgf f/f
Hgf ΔHSC
E
Normal ctrl
ICC Hgf f/f
ICC Hgf ΔHSC
YAP/AKT
CK19
LBR (%)
p=0.064
CK19 area (%)
p=0.0001
F
CGK
P19
Liver
CK19 -
GADPH -
CGKP19 after intrasplenic injection
CGKP19-GFP
CK19
G
Veh
HGF
MzCHA-1
SB1
cells x field
p=0.008
p=0.011
H
Normal ctrl
ICC Hgf f/f
ICC Hgf ΔHSC
YAP/AKT
Ki67
Ki67+ area/tumor
p=0.026
I
CGKP19
+Veh
+HGF
pERK
pAKT
J
MzCHA-1
SB1
CGKP19
T(min) 0 7.5 15 30 60
p-ERK1/2-
ERK1/2-
p-AKT-
AKT-
K
HuCCT-1
CGKP19
U0126 - - - 10 25 50
HGF - + + + + +
p-ERK1/2-
ERK1/2-
L
HSC-CAF
PF-CAF
iCAF
Tumor
HGF
MET
Hu CCA
YAP/AKT ICC2
YAP/AKT ICC3
Expression level
M
Hu CCA
HGF-MET
iCAF/B cell
iCAF/DC-like
iCAF/Endoth
iCAF/Mast
iCAF/Mono
iCAF/Plasma
iCAF/T cell
iCAF/Tumor
Fold
p value

Fig.S7

Figure S7 (Related to Figure 7) | iCAF-derived HGF promotes ICC growth. (A) Representative gating strategy and pictures showing the *Lrat*-Cre^{+}TdTom^{+}*Col1a1*-GFP^{high} (myCAF) and *Lrat*-Cre^{+}TdTom^{+}*Col1a1*-GFP^{low} (iCAF) cells sorted and freshly plated from tumors of KRAS/p19- (n=3) and YAP/AKT-induced ICC (n=2); and ELISA showing that *Lrat*-Cre^{+}TdTom^{+}*Col1a1*-GFP^{low} iCAF produce more HGF compared to the *Lrat*-Cre^{+}TdTom^{+} *Col1a1*-GFP^{high} myCAF 24 hours after plating. Scale bars, 100 μm. (B) Confocal microscopy representative images of RNAscope showing *Has2* and *Hgf* in *Lrat*-Cre^{+}TdTom^{+} mice in KRAS/p19- and YAP/AKT-induced ICC. Scale bars, 50 μm. (C) Representative fluorescent confocal microscopy image of iCAF marker RGS5 and myCAF marker HA and quantifications in human ICC (n=1). Scale bars, 50 μm. (D) *Hgf* mRNA expression in HSC from *Hgf*$^{f/f}$ (n=1) and *Hgf*$^{\Delta HSC}$ (n=2). (E) Representative images of CK19 immunohistochemistry, livers, LBR and CK19^{+} area from *Hgf*$^{f/f}$ (n=9) and *Hgf*$^{\Delta HSC}$(n=8) livers in YAP/AKT-induced ICC. Scale bars 1 cm. (F) CK19 western blot in the CGKP19 cell line (n=1) and whole liver (n=1) and representative picture of liver, CGKP19 native fluorescence and CK19 immunohistochemistry in CGKP19 spleen-injected mouse. Scale bar 100 μm. (G) Human MzCHA-1 and murine SB1 cell lines were treated with recombinant human or mouse HGF (25 ng/ml, n=5) or vehicle (n=5) and cell number was determined after 48h. (H) Representative micrographs of Ki67 IHC in *Hgf*$^{f/f}$ and *Hgf*$^{\Delta HSC}$ in YAP/AKT-induced ICC. Scale bars 100 μm. (I) CGKP19 cells were treated with mouse HGF, followed by phospho-kinase array. (J,K) Human (MzCHA1) and murine (SB1 and CGKP19) CCA cell lines were treated with (J) recombinant HGF (K) in the presence of MEK1/2 inhibitor U0126 or vehicle and were tested by western blot for phosphorylated and total ERK1/2. (L) UMAPs showing the normalized expression levels of *HGF* and *MET* in human CCA (n=1) and in YAP/AKT-induced ICC (n=2). (M) CellphoneDB showing interaction of *HGF*-expressing iCAF with *MET*-expressing cells in human CCA (n=1). For panels A-C,E,G,H; data are shown as mean ± SEM, statistical significance was determined by two-sided unpaired T-test (A,E,G) or Mann-Whitney (B,C) groups of two; and by one-way ANOVA followed by Sidak's posthoc test (E) or Kruskal-Wallis test with Dunn's posthoc test (H) groups of three.

Table S1 (Related to Figure 1 and Figure S1). Description of mouse and human scRNA sequencing samples used for CAF analysis

MOUSE SAMPLES scRNA-seq (GSE154170)

Sample ID	ICC model	Enrichment	HSC-CAF PF-CAF% analysis	iCAF, myCAF, mesCAF% analysis	CellphoneDB analysis	Total CAF number	HSC-CAF number	PF-CAF number	Non-PF, non-HSC other CAF number	iCAF number	myCAF number	mesCAF number	multiCAF number	Non- i/my/ mesCAF other CAF number
YAP/AKT ICC1	YAP/AKT plasmids HDTVI*	100% Col1a1-GFP+	✓	✓	✓	1830	1788	42	none	790	835	41	95	69
YAP/AKT ICC2	YAP/AKT plasmids HDTVI*	70% Col1a1-GFP+ and 30% unpurified tumor suspension	✓	✓	✓	3256	3117	139	none	1747	1026	137	282	64
YAP/AKT ICC3	YAP/AKT plasmids HDTVI*	100% Col1a1-GFP+	✓	✓	✓	4683	4076	607	none	2183	1262	540	563	135
KRAS/p19	KRAS/p19 plasmids HDTVI*	70% Col1a1-GFP+ and 30% unpurified tumor suspension	✓	✓	✓	2662	2324	149	189	1350	686	204	367	55

*HDTVI= Hydrodynamic tail vein injection

HUMAN SAMPLES scRNA-seq

Sample ID	Source paper	Source Sample ID	HSC-CAF PF-CAF% analysis	iCAF, myCAF, mesCAF% analysis	CellphoneDB analysis	Total CAF number	HSC-CAF number	PF-CAF number	Non-PF, non-HSC other CAF number	iCAF number	myCAF number	mesCAF number	multiCAF number	Non- i/my/ mesCAF other CAF number
Human ICC1	Zhang et al., 2020	GSE142784, GSM4240155_ICC24S	✓	✓	✓	2574	2397	177	0	1413	781	144	49	187
Human ICC2-1 *	Zhang et al., 2020	GSE138709, GSM4116585	✓	✓	✓	124	74	50	0	42	21	43	8	10
Human ICC2-2 *	Zhang et al., 2020	GSE138709, GSM4116584	✓	✓	✓	218	199	19	0	98	78	3	34	5
Human ICC2-3	Zhang et al., 2020	GSE138709, GSM4116583	✓	✓	✓	42	42	0	0	24	12	0	6	0
Human ICC2-4	Zhang et al., 2020	GSE138709, GSM4116581				14	14	0	0	2	11	0	0	1
Human ICC2-5	Zhang et al., 2020	GSE138709, GSM4116580				11	11	0	0	6	0	0	0	5
Human ICC3-1	Ma et al., 2019	GSE125449 Set1, S11_P06_LCP29	✓	✓	✓	150	150	0	0	62	37	0	31	20
Human ICC3-2	Ma et al., 2019	GSE125449 Set1, S09_P04_LCP25				24	24	0	0	3	15	0	1	5
Human ICC3-3	Ma et al., 2019	GSE125449 Set1, S08_P03_LCP26				13	13	0	0	2	8	0	1	2
Human ICC3-4	Ma et al., 2019	GSE125449 Set1, S12_P07_LCP30				16	16	0	0	2	10	0	2	2
Human ICC3-5	Ma et al., 2019	GSE125449 Set1, S20_P12_LCP35				37	37	0	0	8	17	0	5	7
Human ICC3-6	Ma et al., 2019	GSE125449 Set1, S19_P11_LCP39				12	12	0	0	1	8	0	3	0
Human ICC4	Zhang et al., 2020	GSE142784, GSM4240156_ICC32S	✓	✓		1228	1228	0	0	905	172	0	72	79

* Different tumors from same patient

Table S2 (Related to Figure 1 and Figure S1). Cell marker genes and signatures for the identification of cell populations in scRNA-seq.

MOUSE CELL POPULATIONS											
PanCAF	*Col1a1*	*Col1a2*	*Col3a1*	*C1s1*	*Acta2*	*C1ra*	*Serpinf1*	*Pdgfrb*	*Col12a1*		
HSC-CAF	*Lrat*	*Des*	*Colec11*	*Rgs5*	*Cygb*	*Ednra*	*Frzb*	*Lum*	*Ndufa4l2*	*Pdgfrb*	*Sept4*
	Tagln										
Global SC-CAF	*Lrp1*	*Marcks*	*Col6a3*	*Cd63*	*Cxcl12*	*Cygb*	*Col5a1*	*Lum*	*Nid1*	*Emp1*	*Tshz2*
PF-CAF	*Msln*	*Upk1b*	*Upk3b*	*Gpm6a*							
Global PF-CAF	*Msln*	*Upk1b*	*Upk3b*	*Gpm6a*	*Krt19*						
Tumor ICC	*Krt19*	*Epcam*									
Endothelial	*Kdr*	*vWf*	*Pecam1*								
Hepatocytes	*Alb*	*Ttr*									
Myeloid	*Adgre1*	*Cd68*	*Cd52*	*Itgam*							
Lymphoid	*Prprcap*	*Cd3e*	*Cd2*	*Cd19*							
emHSC	*Kdr*	*Pecam1*	*Lrat*	*Des*							
Cholangiocytes	*Sctr*	*Hnf1b*	*Krt19*	*Epcam*							
HUMAN CELL POPULATIONS											
PanCAF	*COL1A1*	*COL1A2*	*COL3A1*	*C1S*	*ACTA2*	*C1R*	*SERPINF1*	*PDGFRB*			
HSC	*RGS5*	*LUM*	*COLEC11*	*TAGLN*	*CYGB*	*EDNRA*	*EMILIN1*	*FOXS1*			
	FRZB	*GEM*	*HEYL*	*NDUFA4L2*	*NOTCH3*	*PDGFRB*	*SEPT4*	*SERPINF1*			
	COL14A1	*DCN*									
PF	*MSLN*	*UPK1B*	*KRT19*	*SLPI*							
Tumor ICC	*KRT19*	*EPCAM*									
Endothelial	*KDR*	*VWF*	*ENG*	*AQP1*							
Hepatocyte-like	*ALB*	*TTR*	*APOC3*	*FABP1*	*APOA1*	*FGL1*					
T cell	*CD3E*	*CD3D*	*CD3G*	*CD8A*							
B cell	*CD79A*	*CD79B*	*MS4A1*								
Plasma cell	*JSRP1*	*FCRL5*	*JCHAIN*	*MZB1*	*IGHG3*	*IGHG1*					
Mast cell	*CPA3*	*TPSAB1*	*KIT*								
DC-like cell	*ITGAX*										
Monocytes	*CD68*	*CD74*	*CD14*	*CSF1R*							
Cholangiocytes	*FYXD2*	*TM4SF4*	*ANXA4*	*KRT19*	*EPCAM*						
Macrophages	*VSIG4*	*CD68*	*FCGR2A*	*CD163*							
MOUSE iCAF	*Angptl6*	*C2*	*Cyp27a1*	*Ephb4*	*Gns*	*Ifnar2*	*Lrrc4c*	*Nrxn1*	*Rasgef1b*	*Slc35d1*	*Tmem51*
	Ank3	*C4b*	*Cyr61*	*Etnk1*	*Gpat2*	*Igf1r*	*Ltbp1*	*Nrxn2*	*Rasgrp2*	*Slc40a1*	*Tmem56*
	Ankrd55	*C6*	*Cysltr1*	*Ets1*	*Gpc4*	*Iigp1*	*Ly6e*	*Ntf3*	*Rasl11a*	*Slc4a8*	*Tmem9b*
Aard	*Ano1*	*Cachd1*	*D1Ertd622e*	*Ets2*	*Grap*	*Il10rb*	*Macf1*	*Ntm*	*Rbfox3*	*Slc9a3r2*	*Tmtc2*
Abcc9	*Apoc1*	*Cadm3*	*D430019H16Rik*	*Eva1b*	*Gstm1*	*Il11ra1*	*Man1a*	*Ntn1*	*Rbm46*	*Slco2b1*	*Tnfrsf1 1b*
Abi3bp	*Apoe*	*Calcrl*	*Daam2*	*Fam171b*	*Gstt1*	*Il6st*	*Man2a1*	*P2ry14*	*Rbpms*	*Slco3a1*	*Tnfrsf1b*
Ablim2	*Apold1*	*Camk1d*	*Dapk1*	*Fam26f*	*H2-D1*	*Itga1*	*Map4k3*	*P3h2*	*Rcsd1*	*Slmap*	*Tnfrsf21*
Acap1	*Arap2*	*Ccbe1*	*Dapk2*	*Fam49a*	*H2-K1*	*Itga2b*	*Marcks*	*Pam*	*Reln*	*Smad6*	*Tns1*
Acer2	*Arhgap24*	*Ccdc3*	*Dcdc2a*	*Fam84a*	*H2-Q4*	*Itga9*	*Matn2*	*Papss2*	*Rem1*	*Smagp*	*Tns2*
Acsl5	*Arhgap42*	*Ccdc68*	*Dcn*	*Fbln5*	*H2-Q6*	*Itgb3*	*Mbd2*	*Parp14*	*Rgl1*	*Smpdl3a*	*Tnxb*
Actn4	*Arhgef6*	*Cd302*	*Ddr2*	*Fcna*	*H2-Q7*	*Itih3*	*Mertk*	*Pde1a*	*Rgs2*	*Sntg1*	*Trib2*
Acvr2a	*Arid5b*	*Cdc42ep4*	*Dennd2a*	*Fermt2*	*H6pd*	*Itih4*	*Metrn*	*Pde3a*	*Rgs4*	*Socs3*	*Trim30a*
Adam23	*Arrb1*	*Cdh2*	*Des*	*Fgfr2*	*Hand2*	*Itm2c*	*Mndal*	*Pdgfra*	*Rgs5*	*Sod3*	*Trp53i11*
Adamts1	*Art3*	*Cdk18*	*Dmd*	*Fhl1*	*Hdac7*	*Itpripl1*	*Ms4a4d*	*Pear1*	*Rhobtb1*	*Sorbs1*	*Tshz2*
Adamts10	*Arvcf*	*Cebpb*	*Dock8*	*Filip1l*	*Hes1*	*Jade2*	*Mt1*	*Phactr2*	*Rnaset2b*	*Sox5*	*Tspan7*
Adamts13	*Astn2*	*Chst15*	*Dse*	*Fos*	*Hexim1*	*Jun*	*Mt2*	*Pim1*	*Rock2*	*Sprn*	*Vipr1*
Adamts5	*Atp1a4*	*Cited2*	*Dusp1*	*Fosb*	*Hgf*	*Junb*	*Mtus1*	*Pim3*	*Rspo3*	*Ssfa2*	*Vstm4*
Adamtsl2	*AW112010*	*Cks2*	*Dusp10*	*Foxf1*	*Hhip*	*Jup*	*Mustn1*	*Pkia*	*Rtn1*	*St3gal4*	*Wipf1*
Adap2	*B2m*	*Clca3a1*	*Ece1*	*Frzb*	*Hlx*	*Kcnip3*	*Myc*	*Pla2r1*	*Rtn4rl1*	*Steap4*	*Xdh*
Adap2os	*Bambi*	*Clec14a*	*Ecm1*	*G0s2*	*Hmcn1*	*Kcnj8*	*Mylip*	*Plekha6*	*Rxra*	*Stim1*	*Zbtb16*
Adgrl1	*Bcl2l1*	*Clstn3*	*Ednra*	*Gab1*	*Hpse*	*Klf15*	*Mylk*	*Plscr4*	*Ryk*	*Susd2*	*Zbtb20*
Adm	*Bco1*	*Col14a1*	*Ednrb*	*Gabra3*	*Hs3st3a1*	*Klf9*	*Myo18a*	*Plvap*	*Scarb1*	*Syde1*	*Zfp36*
Adora2a	*Bcr*	*Colec10*	*Efemp1*	*Gdf10*	*Hs3st3b1*	*Ktn1*	*Myo1b*	*Plxnc1*	*Sdc4*	*Syt9*	*Zfp36l1*
Adra2b	*Birc2*	*Colec11*	*Egr1*	*Gdf2*	*Hsd11b1*	*Lama1*	*Ncoa7*	*Ppp1r14a*	*Selenbp1*	*Tbx20*	*Zfp703*
Afap1l2	*Birc3*	*Cp*	*Ehbp1*	*Gem*	*Icam1*	*Ldlrap1*	*Nfia*	*Prelp*	*Sema3d*	*Tcf21*	
Agtr1a	*Bmp10*	*Cped1*	*Ehd3*	*Ggt5*	*Id3*	*Lgals3bp*	*Nfkbia*	*Prex2*	*Sema4b*	*Tgfbi*	
Agtrap	*Bmp2*	*Cpne8*	*Eif4e3*	*Gja4*	*Ier2*	*Lhx2*	*Ngf*	*Prss23*	*Sema6d*	*Tgfbr3*	
Alcam	*Bmp5*	*Crip2*	*Emilin1*	*Gm10600*	*Ifi203*	*Lifr*	*Ngfr*	*Ptafr*	*Serpina3g*	*Tinagl1*	
Aldh1a1	*Bmyc*	*Csf1*	*Eng*	*Gm12216*	*Ifi27l2a*	*Lipa*	*Nkd1*	*Pth1r*	*Serping1*	*Tmem141*	
Aldh1a3	*Bok*	*Ctso*	*Enpp5*	*Gm12840*	*Ifih1*	*Lrat*	*Notch1*	*Ptprk*	*Sft2d2*	*Tmem176a*	
Aldh2	*Btg2*	*Cxcl12*	*Epas1*	*Gm13889*	*Ifit3*	*Lrp4*	*Npr3*	*Ramp1*	*Sgk1*	*Tmem178*	
Alpl	*C1ra*	*Cygb*	*Epb41l2*	*Gm14964*	*Ifitm1*	*Lrp5*	*Nr1h4*	*Ramp2*	*Shisa3*	*Tmem204*	
Angptl2	*C1s1*	*Cyp20a1*	*Epha2*	*Gm37800*	*Ifitm2*	*Lrrc32*	*Nr1h5*	*Raph1*	*Slc29a1*	*Tmem47*	
MOUSE myCAF	*Atxn10*	*Col12a1*	*Ctla2a*	*Fbln1*	*Heyl*	*Lxn*	*Nkd2*	*Pla2g16*	*Rnf19b*	*Slc7a5*	*Tnfaip2*
	Avpi1	*Col15a1*	*Ctxn1*	*Fbln2*	*Hs6st2*	*Maged2*	*Nrep*	*Plat*	*Runx1*	*Smco4*	*Tppp3*
	B4galnt1	*Col1a1*	*Cx3cl1*	*Fbn2*	*Htra1*	*Map1b*	*Nrp2*	*Plaur*	*S100a16*	*Smim3*	*Tsc22d3*
	Bhlhe41	*Col1a2*	*Cxcl14*	*Fgfr1*	*Igfbp5*	*Mapkapk3*	*Nuak1*	*Plod2*	*S100a4*	*Sox4*	*Ttll5*
Ace	*Bmp1*	*Col3a1*	*Cyp51*	*Fkbp11*	*Igsf3*	*Mdfi*	*Ociad2*	*Plp2*	*Sac3d1*	*Sparcl1*	*Tubb2a*

Acot7	*Bpgm*	*Col4a5*	*Dap*	*Frem1*	*Impdh1*	*Mdk*	*Olfml2b*	*Plpp5*	*Scpep1*	*Specc1*	*Tubb3*
Acta2	*Capg*	*Col5a2*	*Dbp*	*Fst*	*Inhba*	*Medag*	*P4ha2*	*Pmepa1*	*Sdc1*	*Spp1*	*Tyms*
Actg2	*Cd59a*	*Col5a3*	*Ddah1*	*Fstl1*	*Itm2a*	*Meox1*	*Pafah1b3*	*Podxl2*	*Serf1*	*Srpx*	*Uck2*
Adam19	*Cd9*	*Col6a2*	*Dpysl3*	*Fstl3*	*Kctd11*	*Mfap2*	*Palld*	*Prrx1*	*Serpine2*	*Stc2*	*Vcan*
Adcy7	*Cd93*	*Col7a1*	*Ebf1*	*Fxyd5*	*Kdelr3*	*Mfap4*	*Pcbp4*	*Prss35*	*Serpinf1*	*Stk17b*	*Vegfa*
Ahnak2	*Cda*	*Col8a1*	*Egln3*	*Fxyd6*	*Kif26b*	*Mgll*	*Pdgfrl*	*Ptgfrn*	*Sesn3*	*Sulf1*	*Vmp1*
Ak1	*Cdh11*	*Colec12*	*Emp1*	*Fzd1*	*Kremen1*	*Mgp*	*Pdlim3*	*Ptk7*	*Sfrp1*	*Tfpi2*	*Wisp1*
Akr1b8	*Cdkn2a*	*Comtd1*	*Eno1*	*Gas7*	*Lama4*	*Mical2*	*Pdzrn3*	*Ptn*	*Sh3bgrl3*	*Tgfb3*	*Wnt11*
Aldh1a2	*Cdkn2b*	*Copz2*	*Enpp1*	*Gm15867*	*Lef1*	*Minos1*	*Pgam1*	*Ptprb*	*Sh3pxd2b*	*Thy1*	*Zswim7*
Ank	*Cercam*	*Cotl1*	*Etv4*	*Gng11*	*Lefty1*	*Mmp14*	*Pgf*	*Rab7b*	*Shisa4*	*Thyn1*	
Ankrd37	*Ch25h*	*Cox4i2*	*Evl*	*Gpbar1*	*Lgals1*	*Mmp2*	*Pgk1*	*Rap2b*	*Siva1*	*Timp1*	
Anpep	*Chst11*	*Cpxm2*	*Fam198b*	*Gpc1*	*Lgi2*	*Mtch1*	*Piezo2*	*Rapgef4*	*Slc16a3*	*Tm4sf1*	
Aoc1	*Chst2*	*Crlf1*	*Fam20a*	*Gpm6b*	*Lhfpl2*	*Nbl1*	*Pik3ip1*	*Rgs16*	*Slc27a1*	*Tmem2*	
Apol9a	*Clec11a*	*Csrp2*	*Fam20c*	*Gpr153*	*Lsp1*	*Ncam1*	*Pkm*	*Rgs19*	*Slc39a14*	*Tmem45a*	
Aprt	*Clmp*	*Cthrc1*	*Fam69b*	*H1f0*	*Ltbp2*	*Ndufa4l2*	*Pla1a*	*Rnf149*	*Slc7a2*	*Tnc*	
MOUSE mesCAF											
Adgrd1	*Cd2ap*	*Flrt2*	*Igfbp6*	*Mmd*	*Rbbp8*	*Slc9a3r1*	*Tmem98*				
Angptl7	*Celf2*	*Fth1*	*Il18*	*Msln*	*Rspo1*	*Slpi*	*Tnfaip3*				
Anxa3	*Cpe*	*Gas6*	*Krt18*	*Ndrg1*	*S100a1*	*Smpd3*	*Tnfrsf12a*				
Atp1b1	*Cxadr*	*Gm20186*	*Krt7*	*Ndufa4*	*Saa3*	*Snrpg*	*Trf*				
Bicd1	*Dab2*	*Gm8186*	*Krt8*	*Nkain4*	*Sbsn*	*Spint2*	*Ucp2*				
C3	*Ddr1*	*Gpc3*	*Ldhb*	*Pdgfc*	*Serpinb6b*	*Stmn1*	*Upk1b*				
Cd151	*Ezr*	*Gpm6a*	*Lgals3*	*Pdpn*	*Shb*	*Tcea3*	*Upk3b*				
Cd200	*Fbxo33*	*Hspb1*	*Lrrn4*	*Rab11a*	*Slc39a8*	*Tmem151a*	*Wt1*				
HUMAN iCAF											
ADAMTS4	*AGT*	*APOE*	*ARHGDIB*	*CCL19*	*CCL21*	*COLEC11*	*CPE*	*GEM*	*GJA4*		
GPX3	*HIGD1B*	*IL6*	*ISYNA1*	*LHFP*	*MAP1B*	*MT1A*	*NDUFA4L2*	*PDK4*	*RGS5*		
HUMAN myCAF											
APOD	*CCL11*	*COL1A1*	*COL1A2*	*COL3A1*	*COL5A1*	*COL6A3*	*CTGF*	*CTHRC1*	*CYP1B1*	*FN1*	
INHBA	*ISLR*	*LUM*	*MMP14*	*POSTN*	*PTGDS*	*SERPINF1*	*SFRP2*	*SPON2*	*VCAN*		
HUMAN mesCAF											
ANXA1	*ANXA2*	*BDKRB1*	*C19orf33*	*C3*	*CALB2*	*CCDC80*	*CFB*	*CRABP2*			
CXCL1	*CXCL6*	*EFEMP1*	*EGFL6*	*EMP3*	*EZR*	*HMOX1*	*HP*	*HSPA6*			
IFI27	*IGFBP6*	*ITLN1*	*KRT18*	*KRT19*	*KRT8*	*LINC01133*	*LOX*	*MT1E*			
MT1G	*MT1X*	*MXRA5*	*PDPN*	*PLA2G2A*	*PRG4*	*PRSS23*	*PTGIS*	*RP11-572C15.6*			
S100A10	*S100A16*	*S100A6*	*SAA1*	*SAA2*	*SERPINE2*	*SH3BGRL3*	*SLC12A8*	*SLPI*	*TM4SF1*		

Table S3 (Related to Figure 1). Functional enrichment analysis in HSC from BDL (n=4) and DDC (n=4) fibrosis models and HSC-CAF from YAP/AKT- (n=4) and KRAS/p19- (n=3) induced ICC models using g:Profiler.

term_name	term_id	term_size	effective domain size	adjusted p value HSC BDL	query size HSC BDL	intersection size HSC BDL	query size HSC DDC	intersection size HSC DDC	adjusted p value CAF YAP/AKT	query size CAF YAP/AKT	intersection size CAF YAP/AKT	adjusted p value CAF KRAS/p19	query size CAF KRAS/p19	intersection size CAF KRAS/p19
extracellular region	GO:0005576	2804	21259	7.77E-08	99	38	80	35	2.67E-08	96	38	5.89E-16	75	42
extracellular matrix	GO:0031012	487	21259	1.03658E-06	94	15	57	11	1.83E-07	59	13	6.47E-10	79	17
extracellular space	GO:0005615	1941	21259	2.98E-07	51	21	79	26	2.15041E-05	96	27	4.99E-08	70	26
collagen-containing extracellular matrix	GO:0062023	359	21259	1.78404E-05	94	12	36	8	7.10E-08	59	12	1.83E-07	94	14
signaling receptor binding	GO:0005102	1780	21091	1	70	14	74	12	0.002845884	91	22	2.71163E-06	86	26
extracellular matrix structural constituent	GO:0005201	133	21091	4.41113E-06	94	9	25	4	0.001105235	59	6	1.96906E-05	79	8
tube development	GO:0035295	1140	21354	1	84	13	54	13	0.000151874	68	17	4.79798E-05	49	15
kidney development	GO:0001822	327	21354	1	58	5	46	7	3.04957E-05	73	11	0.000113061	49	9
renal system development	GO:0072001	337	21354	1	58	5	46	7	4.15614E-05	73	11	0.000146254	49	9
ossification	GO:0001503	394	21354	1	94	6	46	7	0.000783761	83	11	0.000184979	57	10
animal organ morphogenesis	GO:0009887	1045	21354	1	99	13	46	8	0.03129489	85	15	0.000330507	86	18
urogenital system development	GO:0001655	380	21354	1	79	6	46	7	0.000141373	73	11	0.000405537	49	9
biomineral tissue development	GO:0031214	160	21354	1	94	4	46	5	0.004236973	50	6	0.000450113	56	7
biomineralization	GO:0110148	162	21354	1	94	4	46	5	0.004554113	50	6	0.000489848	56	7
xenobiotic glucuronidation	GO:0052697	9	21354	0.957878873	1	1	5	2	0.000172614	22	3	0.000579999	32	3
flavonoid glucuronidation	GO:0052696	9	21354	0.957878873	1	1	5	2	0.000172614	22	3	0.000579999	32	3
anatomical structure morphogenesis	GO:0009653	2730	21354	0.003295181	100	31	96	25	2.31458E-05	87	32	0.000604815	98	32
tissue development	GO:0009888	1963	21354	0.203447015	100	22	88	25	1.047E-05	85	27	0.000616129	72	22
microfibril	GO:0001527	11	21259	0.003891102	94	3	25	2	0.017692828	23	2	0.000842584	56	3
animal organ development	GO:0048513	3628	21354	0.06226051	100	34	94	30	0.000148434	87	36	0.001337753	68	29
extracellular matrix organization	GO:0030198	289	21354	0.019821241	100	9	34	4	1	61	5	0.001390976	73	9
extracellular structure organization	GO:0043062	291	21354	0.020947287	100	9	34	4	1	61	5	0.001473328	73	9
hormone catabolic process	GO:0042447	11	21354	0.689495347	51	2	30	2	0.143853547	24	2	0.001499023	35	3
cellular glucuronidation	GO:0052695	12	21354	1	1	1	5	2	0.000451181	22	3	0.001514408	32	3
tube morphogenesis	GO:0035239	916	21354	1	84	9	54	8	0.001996834	68	14	0.001746287	49	12
uronic acid metabolic process	GO:0006063	13	21354	1	1	1	5	2	0.000586144	22	3	0.001966726	32	3
glucuronate metabolic process	GO:0019585	13	21354	1	1	1	5	2	0.000586144	22	3	0.001966726	32	3
flavonoid metabolic process	GO:0009812	14	21354	1	1	1	5	2	0.000745503	22	3	0.002500557	32	3
osteoblast differentiation	GO:0001649	207	21354	1	94	4	46	6	0.035164389	83	7	0.002895903	57	7
xenobiotic metabolic process	GO:0006805	103	21354	0.82615765	29	3	81	5	0.007592701	22	4	0.00410986	76	6
cell motility	GO:0048870	1655	21354	0.023308881	81	19	90	19	0.000347167	63	19	0.004956436	87	21
localization of cell	GO:0051674	1655	21354	0.023308881	81	19	90	19	0.000347167	63	19	0.004956436	87	21
cellular response to xenobiotic stimulus	GO:0071466	107	21354	0.923846369	29	3	81	5	0.008838458	22	4	0.005136614	76	6
lung development	GO:0030324	213	21354	1	44	3	46	5	0.000826155	68	8	0.006033851	40	6
bone trabecula formation	GO:0060346	11	21354	1	94	1	33	2	0.76728063	55	2	0.006311414	56	3
respiratory tube development	GO:0030323	216	21354	1	44	3	46	5	0.000918758	68	8	0.006541655	40	6
muscle cell migration	GO:0014812	109	21354	0.000430462	81	7	85	5	0.027612405	59	5	0.007187338	79	6
locomotion	GO:0040011	1845	21354	0.00805022	81	21	90	19	0.001856186	63	19	0.007442679	87	22
morphogenesis of an epithelium	GO:0002009	541	21354	1	100	6	46	6	0.046970783	61	9	0.007617839	49	9
Drug metabolism - cytochrome P450	KEGG:00982	67	8477	0.446592765	15	2	12	3	0.001712385	22	4	0.007863115	32	4
system development	GO:0048731	4897	21354	0.081793495	90	38	94	37	0.000411564	87	42	0.007866464	98	43
response to xenobiotic stimulus	GO:0009410	116	21354	1	29	3	81	5	0.012188862	22	4	0.008222982	76	6
cell adhesion	GO:0007155	1377	21354	1	89	14	96	16	0.011759839	61	15	0.008264717	98	20
receptor regulator activity	GO:0030545	564	21091	0.03206153	81	10	74	7	0.091408454	91	10	0.008783806	85	11
biological adhesion	GO:0022610	1389	21354	1	89	14	96	16	0.013066337	61	15	0.009420014	98	20
insulin-like growth factor binding protein complex	GO:0016942	5	21259	0.01559776	50	2	78	2	0.013183482	46	2	0.010298155	40	2
growth factor complex	GO:0036454	5	21259	0.01559776	50	2	78	2	0.013183482	46	2	0.010298155	40	2
ECM-receptor interaction	KEGG:04512	87	8477	0.698112296	81	4	36	4	0.024005755	59	5	0.010860404	79	6
glucuronosyltransferase activity	GO:0015020	35	21091	0.901888916	1	1	5	2	0.003625847	22	3	0.010918447	32	3
Extracellular matrix organization	REAC: R-MMU-1474244	253	8684	1	94	8	36	6	0.088534638	33	6	0.011737981	73	10
respiratory system development	GO:0060541	242	21354	1	44	3	46	5	0.000406577	99	10	0.012580169	40	6
Ascorbate and aldarate metabolism	KEGG:00053	30	8477	0.26137281	1	1	5	2	0.00430337	22	3	0.013415364	32	3
bone trabecula morphogenesis	GO:0061430	14	21354	1	94	1	33	2	1	55	2	0.013845801	56	3
epithelium development	GO:0060429	1173	21354	1	100	11	67	11	0.00276825	80	17	0.014752797	55	13
Regulation of Insulin-like Growth Factor (IGF) transport and uptake by Insulin-like Growth Factor Binding Proteins (IGFBPs)	REAC: R-MMU-381426	111	8684	0.491558526	69	5	78	5	0.282680893	91	6	0.015390505	54	6
cell migration	GO:0016477	1499	21354	0.022818416	81	18	90	18	7.24863E-05	63	19	0.016551988	51	14
Glucuronidation	REAC: R-MMU-156588	22	8684	0.681020094	1	1	5	2	0.005663518	22	3	0.01720389	32	3
anatomical structure formation involved in morphogenesis	GO:0048646	1174	21354	1	100	13	54	8	0.000289436	85	19	0.018422674	56	13
vasculature development	GO:0001944	774	21354	1	84	9	54	7	0.064391429	80	12	0.019139181	49	10
Pentose and glucuronate interconversions	KEGG:00040	34	8477	0.296222518	1	1	5	2	0.006300168	22	3	0.019571028	32	3
Porphyrin and chlorophyll metabolism	KEGG:00860	41	8477	0.357209507	1	1	5	2	0.011091865	22	3	0.019807753	66	4
hormone metabolic process	GO:0042445	207	21354	1	51	3	40	4	1	91	5	0.020497252	76	7
multicellular organism development	GO:0007275	5474	21354	0.985436356	90	38	98	39	0.001140113	87	44	0.024777103	98	45
Metabolism of xenobiotics by cytochrome P450	KEGG:00980	69	8477	0.601157463	1	1	12	3	0.052009646	22	3	0.026409616	76	5
negative regulation of canonical Wnt signaling pathway	GO:0090090	130	21354	1	-1	-1	46	2	0.764584367	55	4	0.027060572	49	5
mesenchymal cell differentiation	GO:0048762	224	21354	1	100	2	46	4	0.045893914	80	7	0.02717077	49	6
cell-substrate adhesion	GO:0031589	352	21354	1	100	4	36	4	0.015057786	61	8	0.027776319	86	9
regulation of insulin-like growth factor receptor signaling pathway	GO:0043567	25	21354	0.060887854	50	3	78	3	0.04524633	46	3	0.030930508	40	3
Molecules associated with elastic fibres	REAC: R-MMU-2129379	31	8684	1	94	3	25	2	0.800531969	23	2	0.031389939	73	4
tissue morphogenesis	GO:0048729	646	21354	1	80	8	46	7	0.156845386	35	7	0.031757042	49	9
extracellular matrix binding	GO:0050840	57	21091	1	81	2	19	1	0.84786404	83	3	0.033659128	79	4
regulation of cell population proliferation	GO:0042127	1769	21354	1	100	18	46	9	0.012962412	61	17	0.035072177	85	20
response to steroid hormone	GO:0048545	357	21354	0.352046241	92	8	82	7	0.136413053	81	8	0.035421997	67	8
bone mineralization	GO:0030282	121	21354	1	94	3	77	5	0.012597371	79	6	0.037041945	56	5
negative regulation of transmembrane receptor protein serine/threonine kinase signaling pathway	GO:0090101	121	21354	1	94	3	33	4	0.177316285	78	5	0.037041945	56	5
UDP-glycosyltransferase activity	GO:0008194	152	21091	1	1	1	5	2	0.161657094	44	4	0.043306072	32	4
regulation of osteoblast differentiation	GO:0045667	140	21354	1	94	3	38	3	1	83	4	0.046331832	85	6
frizzled binding	GO:0005109	41	21091	1	-1	-1	46	2	0.095831946	55	3	0.046432783	44	3
negative regulation of cell population proliferation	GO:0008285	701	21354	1	100	8	46	5	0.344383342	61	9	0.047554559	85	12
response to glucocorticoid	GO:0051384	180	21354	0.293480918	92	6	82	5	1	81	4	0.048870196	67	6
receptor antagonist activity	GO:0048019	16	21091	1	17	1	13	1	0.262303735	42	2	0.049767759	19	2
movement of cell or subcellular component	GO:0006928	2087	21354	0.004169579	81	23	94	20	0.003581921	64	20	0.053095402	87	22
Retinol metabolism	KEGG:00830	94	8477	0.818968138	1	1	87	7	0.037258981	34	4	0.056831852	38	4
regulation of developmental process	GO:0050793	2602	21354	1	100	22	94	18	0.014842244	91	27	0.061521797	87	25
regulation of anatomical structure morphogenesis	GO:0022603	964	21354	1	100	9	94	9	0.032761011	61	12	0.075495818	87	14
regulation of smooth muscle cell migration	GO:0014910	89	21354	0.000341529	58	6	81	4	1	44	3	0.083776119	45	4
Steroid hormone biosynthesis	KEGG:00140	88	8477	0.766693576	1	1	87	6	0.105508027	22	3	0.08461788	45	4
response to organic cyclic compound	GO:0014070	1047	21354	0.037148453	96	16	82	14	1	91	13	0.095676914	72	13
Estrogen metabolism	WP:WP1264	12	4470	0.094734579	29	2	1	1	0.005026694	7	2	0.09797678	1	1
cell population proliferation	GO:0008283	2086	21354	1	100	20	46	10	0.028559649	61	18	0.098895107	72	19
regulation of cell migration	GO:0030334	940	21354	1	81	11	86	10	0.025463729	61	12	0.101773518	49	10
regulation of cell motility	GO:2000145	991	21354	1	81	11	86	10	0.043107812	61	12	0.101987901	87	14
response to endogenous stimulus	GO:0009719	1620	21354	0.001310278	96	23	38	11	0.007321111	91	21	0.102785427	69	16
smooth muscle cell migration	GO:0014909	96	21354	0.000536936	58	6	81	4	1	44	3	0.112764486	45	4
Chemical carcinogenesis	KEGG:05204	96	8477	0.836392992	1	1	87	7	0.135541232	22	3	0.116884877	45	4
Glucuronidation	WP:WP1241	15	4470	0.123371496	1	1	5	2	0.001654449	22	3	0.122470974	1	1
developmental process	GO:0032502	6586	21354	1	100	46	98	42	0.004508178	87	48	0.127787039	98	49
anatomical structure development	GO:0048856	6028	21354	1	100	44	98	41	0.002380422	87	46	0.140332198	98	46
cellular response to chemical stimulus	GO:0070887	3111	21354	0.422218876	51	18	43	18	0.014207187	86	29	0.161137749	87	27
basement membrane	GO:0005604	109	21259	1	81	3	36	2	0.002913959	96	6	0.218878191	79	4
cell morphogenesis	GO:0000902	1062	21354	1	81	9	94	11	0.002443341	87	17	0.219828306	98	15
regulation of establishment of planar polarity	GO:0090175	44	21354	1	-1	-1	46	2	0.003956652	99	5	0.231594181	44	3
regulation of cellular component movement	GO:0051270	1077	21354	1	81	12	86	10	0.032932896	64	13	0.248381317	87	14

epithelial cell proliferation	GO:0050673	429	21354	1	81	6	38	5	0.005504332	59	9	0.26239298	94	9
ovulation cycle	GO:0042698	84	21354	0.003359416	90	6	34	1	1	50	3	0.268790672	64	4
Drug metabolism - other enzymes	KEGG:00983	88	8477	0.766693576	1	1	12	3	0.105508027	22	3	0.312597491	32	3
response to organic substance	GO:0010033	3434	21354	0.054186759	96	32	41	18	0.02613305	85	30	0.339735166	87	28
retinoic acid binding	GO:0001972	16	21091	0.412292076	1	1	1	1	0.006497501	7	2	0.412292076	1	1
response to vitamin D	GO:0033280	34	21354	1	73	2	33	2	0.028210783	91	4	0.463704759	72	3
enzyme linked receptor protein signaling pathway	GO:0007167	918	21354	1	50	8	45	8	0.030949112	96	15	0.615961375	85	12
establishment of planar polarity	GO:0001736	63	21354	1	-1	-1	46	2	0.023886084	99	5	0.675713007	44	3
establishment of tissue polarity	GO:0007164	64	21354	1	-1	-1	46	2	0.025815633	99	5	0.707927442	44	3
organic acid metabolic process	GO:0006082	948	21354	1	100	12	59	13	1	73	10	0.711685349	50	9
response to nutrient	GO:0007584	191	21354	1	73	4	35	5	0.038299754	91	7	0.820203001	38	4
retinoid binding	GO:0005501	34	21091	0.876120661	1	1	35	2	6.39148E-05	73	5	0.876120661	1	1
cellular response to organic substance	GO:0071310	2461	21354	0.074678934	51	17	41	16	0.142191115	85	23	0.88319428	72	19
response to vitamin	GO:0033273	105	21354	1	73	2	35	3	0.012639842	91	6	0.998213458	72	4
isoprenoid binding	GO:0019840	39	21091	1	1	1	1	1	0.000130485	73	5	1	1	1
oxidoreductase activity, acting on paired donors, with incorporation or reduction of molecular oxygen	GO:0016705	221	21091	0.930457494	82	5	87	7	1	73	2	1	80	4
hyaluronan synthase activity	GO:0050501	4	21091	0.024150363	58	2	34	1	1	44	1	1	26	1
monooxygenase activity	GO:0004497	160	21091	1	29	2	87	6	1	73	2	1	76	3
cell morphogenesis involved in differentiation	GO:0000904	767	21354	1	76	7	94	10	0.00096158	87	15	1	98	11
midgut development	GO:0007494	12	21354	1	19	1	51	3	1	34	1	1	97	2
cellular response to growth factor stimulus	GO:0071363	671	21354	1	94	8	34	6	0.029504316	85	12	1	71	8
cellular response to endogenous stimulus	GO:0071495	1329	21354	0.315544868	48	11	38	10	0.034857925	85	17	1	64	11
cell development	GO:0048468	2361	21354	1	90	17	86	14	0.035493224	87	24	1	98	21
rhythmic process	GO:0048511	347	21354	0.035959652	90	9	83	2	1	82	5	1	64	4
monocarboxylic acid metabolic process	GO:0032787	616	21354	1	100	9	95	12	1	73	8	1	50	7
response to extracellular stimulus	GO:0009991	566	21354	1	6	2	72	10	1	55	7	1	38	6
digestive tract development	GO:0048565	138	21354	1	19	1	51	5	1	68	4	1	38	3
response to growth factor	GO:0070848	698	21354	1	58	6	34	6	0.043605217	85	12	1	71	8
extracellular polysaccharide metabolic process	GO:0046379	3	21354	0.049348422	58	2	34	1	1	44	1	1	26	1
extracellular polysaccharide biosynthetic process	GO:0045226	3	21354	0.049348422	58	2	34	1	1	44	1	1	26	1
Factor: GLI; motif: NSTGGGTGGTCY	TF:M10254	9881	21859	1	94	53	90	61	0.022650143	82	56	1	90	55
Factor: Smad2; motif: NCTGYCTGN	TF:M10366	6664	21859	1	82	37	88	45	1	95	40	1	45	22

Table S4 (Related to Figures 4, S4). Functional enrichment analysis in mouse iCAF common to YAP/AKT- and KRAS/p19-induced ICC models performed using g:Profiler.

term_name	term id	adjusted p value	negative log10 of adjusted p value	term size	query size	intersection size	effective domain size	intersections
growth factor activity	GO:0008083	0.000405722	3.391771912	146	48	6	21095	BMP10,GDF2,GDF10,CXCL12,HGF,NTF3
receptor ligand activity	GO:0048018	0.007654147	2.116103185	511	48	8	21095	COLEC10,BMP10,GDF2,NTN1,GDF10,CXCL12,HGF,NTF3
signaling receptor activator activity	GO:0030546	0.008208415	2.085740708	516	48	8	21095	COLEC10,BMP10,GDF2,NTN1,GDF10,CXCL12,HGF,NTF3
receptor regulator activity	GO:0030545	0.013810205	1.859799868	555	48	8	21095	COLEC10,BMP10,GDF2,NTN1,GDF10,CXCL12,HGF,NTF3
pattern recognition receptor activity	GO:0038187	0.01459221	1.835878931	19	10	2	21095	FCNA,PTAFR
signaling receptor binding	GO:0005102	0.038987429	1.409075408	1731	48	13	21095	COLEC10,BMP10,NRXN1,GDF2,RELN,RSPO3,EDNRB,NTN1,GDF10,CXCL12 ITGB3,HGF,NTF3
cytokine activity	GO:0005125	0.042344579	1.373202184	235	42	5	21095	BMP10,GDF2,NTN1,GDF10,CXCL12
chemoattractant activity	GO:0042056	0.046997084	1.327929084	41	48	3	21095	COLEC10,HGF,NTF3
chemotaxis	GO:0006935	0.000112748	3.947892433	594	48	11	21257	COLEC10,PTAFR,RELN,SUCNR1,EDNRB,NTN1,CXCL12,ANK3,ITGB3,HGF,NTF3
taxis	GO:0042330	0.000118647	3.925741441	597	48	11	21257	COLEC10,PTAFR,RELN,SUCNR1,EDNRB,NTN1,CXCL12,ANK3,ITGB3,HGF,NTF3
angiogenesis	GO:0001525	0.000326728	3.485813022	529	47	10	21257	HHIP,NRXN1,GDF2,ANGPTL6,C6,RSPO3,CXCL12,RAMP1,ITGB3,HGF
cellular response to chemical stimulus	GO:0070887	0.000346721	3.460019276	3087	48	22	21257	HHIP,BMP10,NRXN1,GDF2,PTAFR,NR1H5,PDE8B,LRAT,EDNRB,PLVAP,ALPL,NTN1,DOCK8,GDF10,ADAMTS13,SOD3,CXCL12,ANK3,RAMP1,ITGB3,HGF, NTF3
blood vessel development	GO:0001568	0.000659488	3.18079318	725	47	11	21257	HHIP,NRXN1,GDF2,ANGPTL6,C6,RSPO3,GJA4,CXCL12,RAMP1,ITGB3,HGF
positive regulation of multicellular organismal process	GO:0051240	0.000709835	3.148842734	1905	48	17	21257	BMP10,NRXN1,FCNA,GDF2,PTAFR,RELN,C6,EDNRB,CLSTN3,ADRA2B,NTN1, GDF10,MUSTN1,CXCL12,ITGB3,HGF,NTF3
vasculature development	GO:0001944	0.000985148	3.006498521	755	47	11	21257	HHIP,NRXN1,GDF2,ANGPTL6,C6,RSPO3,GJA4,CXCL12,RAMP1,ITGB3,HGF
cellular response to organic substance	GO:0071310	0.001148848	2.939737255	2472	48	19	21257	HHIP,BMP10,NRXN1,GDF2,PTAFR,NR1H5,PDE8B,LRAT,EDNRB,PLVAP,ALPL, DOCK8,GDF10,ADAMTS13,CXCL12,RAMP1,ITGB3,HGF,NTF3
cardiovascular system development	GO:0072358	0.001150901	2.938961887	767	47	11	21257	HHIP,NRXN1,GDF2,ANGPTL6,C6,RSPO3,GJA4,CXCL12,RAMP1,ITGB3,HGF
positive regulation of locomotion	GO:0040017	0.001398235	2.854419913	606	48	10	21257	PTAFR,RELN,SUCNR1,PLVAP,NTN1,DOCK8,CXCL12,ITGB3,HGF,NTF3
blood vessel morphogenesis	GO:0048514	0.001569884	2.804132465	628	47	10	21257	HHIP,NRXN1,GDF2,ANGPTL6,C6,RSPO3,CXCL12,RAMP1,ITGB3,HGF
locomotion	GO:0040011	0.001800323	2.744649689	1796	48	16	21257	COLEC10,BMP10,GDF2,PTAFR,RELN,SUCNR1,DCDC2A,EDNRB,PLVAP,NTN1, DOCK8,CXCL12,ANK3,ITGB3,HGF,NTF3
regulation of locomotion	GO:0040012	0.004013247	2.396504095	1037	48	12	21257	BMP10,GDF2,PTAFR,RELN,SUCNR1,PLVAP,NTN1,DOCK8,CXCL12,ITGB3,HGF,NTF3
cell adhesion	GO:0007155	0.004074403	2.389936059	1298	46	13	21257	COLEC10,BMP10,NRXN1,PTAFR,RELN,NTM,CLSTN3,NTN1,DOCK8,CXCL12, ANK3, ITGB3,CADM3
biological adhesion	GO:0022610	0.004474102	2.349294129	1309	46	13	21257	COLEC10,BMP10,NRXN1,PTAFR,RELN,NTM,CLSTN3,NTN1,DOCK8,CXCL12, ANK3,ITGB3,CADM3
tube morphogenesis	GO:0035239	0.005013173	2.299887297	892	47	11	21257	HHIP,NRXN1,GDF2,ANGPTL6,C6,RSPO3,NTN1,CXCL12,RAMP1,ITGB3,HGF
multicellular organism development	GO:0007275	0.006020239	2.2203863	5293	48	27	21257	HHIP,COLEC10,BMP10,NRXN1,GDF2,ANGPTL6,RELN,NR1H5,SHISA3,NTM,C6, RSPO3,DCDC2A,EDNRB,CLSTN3,SLCO2B1,ADRA2B,ALPL,GJA4,NTN1,MUSTN1,CXCL12,ANK3,RAMP1,ITGB3,HGF,NTF3
NMDA glutamate receptor clustering	GO:0097114	0.006289006	2.201418014	6	11	2	21257	NRXN1,RELN
tube development	GO:0035295	0.006316468	2.199525686	1109	47	12	21257	HHIP,NRXN1,GDF2,ANGPTL6,C6,RSPO3,EDNRB,NTN1,CXCL12,RAMP1,ITGB3,HGF
positive regulation of developmental process	GO:0051094	0.007425993	2.129245452	1526	48	14	21257	BMP10,NRXN1,GDF2,RELN,C6,CLSTN3,ADRA2B,NTN1,GDF10,MUSTN1,CXCL12, ITGB3,HGF,NTF3
regulation of cell migration	GO:0030334	0.007659186	2.115817398	911	48	11	21257	BMP10,GDF2,PTAFR,RELN,PLVAP,NTN1,DOCK8,CXCL12,ITGB3,HGF,NTF3
positive regulation of cell motility	GO:2000147	0.008334152	2.079138596	576	48	9	21257	PTAFR,RELN,PLVAP,NTN1,DOCK8,CXCL12,ITGB3,HGF,NTF3
circulatory system development	GO:0072359	0.008850349	2.053039622	1146	47	12	21257	HHIP,BMP10,NRXN1,GDF2,ANGPTL6,C6,RSPO3,GJA4,CXCL12,RAMP1,ITGB3,HGF
anatomical structure formation involved in morphogenesis	GO:0048646	0.009009862	2.045281861	1148	47	12	21257	HHIP,BMP10,NRXN1,GDF2,ANGPTL6,RELN,C6,RSPO3,CXCL12,RAMP1,ITGB3,HGF
cell-cell adhesion	GO:0098609	0.010130559	1.994366569	792	46	10	21257	COLEC10,NRXN1,PTAFR,CLSTN3,NTN1,DOCK8,CXCL12,ANK3,ITGB3,CADM3
positive regulation of cellular component movement	GO:0051272	0.011434139	1.941796534	599	48	9	21257	PTAFR,RELN,PLVAP,NTN1,DOCK8,CXCL12,ITGB3,HGF,NTF3
cell surface receptor signaling pathway	GO:0007166	0.011746087	1.930106779	2655	11	8	21257	HHIP,BMP10,NRXN1,VIPR1,FCNA,GDF2,PTAFR,RELN
positive regulation of response to stimulus	GO:0048584	0.012201051	1.913602772	2338	48	17	21257	BMP10,NRXN1,FCNA,GDF2,PTAFR,RELN,SUCNR1,C6,RSPO3,DCDC2A,ADRA2B GDF10,COLEC11,CXCL12,ITGB3,HGF,NTF3
regulation of cell motility	GO:2000145	0.012864465	1.890608275	962	48	11	21257	BMP10,GDF2,PTAFR,RELN,PLVAP,NTN1,DOCK8,CXCL12,ITGB3,HGF,NTF3
multicellular organismal process	GO:0032501	0.013902752	1.856899226	8304	48	34	21257	HHIP,COLEC10,BMP10,NRXN1,FCNA,GDF2,ANGPTL6,PTAFR,RELN,NR1H5,SHISA3, NTM,SUCNR1,PDE8B,C6,RSPO3,LRAT,DCDC2A,EDNRB,CLSTN3,SLCO2B1,ADRA2B,APLL,GJA4,NTN1,GDF10,ADAMTS13,MUSTN1,CXCL12,ANK3,RAMP1,ITGB3,HGF,NTF3
positive regulation of nervous system process	GO:0031646	0.014833453	1.828757734	81	11	3	21257	NRXN1,PTAFR,RELN
anatomical structure morphogenesis	GO:0009653	0.017256127	1.76305666	2673	48	18	21257	HHIP,BMP10,NRXN1,GDF2,ANGPTL6,RELN,C6,RSPO3,DCDC2A,ALPL,NTN1, MUSTN1,CXCL12,ANK3,RAMP1,ITGB3,HGF,NTF3
positive regulation of synapse maturation	GO:0090129	0.018845722	1.724787211	10	11	2	21257	NRXN1,RELN
regulation of multicellular organismal development	GO:2000026	0.019038939	1.72035726	2152	48	16	21257	HHIP,BMP10,NRXN1,GDF2,RELN,NTM,C6,EDNRB,CLSTN3,ADRA2B,NTN1,MUSTN1, CXCL12,ITGB3,HGF,NTF3
multicellular organismal response to stress	GO:0033555	0.021084474	1.676037221	95	32	4	21257	RELN,PDE8B,EDNRB,GJA4
regulation of fibroblast growth factor receptor signaling pathway	GO:0040036	0.02125359	1.672567697	31	4	2	21257	HHIP,NRXN1
cell migration	GO:0016477	0.021274374	1.672143218	1440	48	13	21257	BMP10,GDF2,PTAFR,RELN,DCDC2A,EDNRB,PLVAP,NTN1,DOCK8,CXCL12,ITGB3, HGF,NTF3
postsynaptic density protein 95 clustering	GO:0097119	0.023027159	1.637759648	11	11	2	21257	NRXN1,RELN
developmental process	GO:0032502	0.023060343	1.637134235	6410	48	29	21257	HHIP,COLEC10,BMP10,NRXN1,GDF2,ANGPTL6,RELN,NR1H5,SHISA3,NTM,C6, RSPO3,DCDC2A,EDNRB,STEAP4,CLSTN3,SLCO2B1,ADRA2B,ALPL,GJA4,NTN1,GDF10, MUSTN1,CXCL12,ANK3,RAMP1,ITGB3,HGF,NTF3
regulation of response to stimulus	GO:0048583	0.025665761	1.590645848	3962	48	22	21257	HHIP,BMP10,NRXN1,FCNA,GDF2,PTAFR,RELN,RGS5,SUCNR1,PDE8B,C6,RSPO3, DCDC2A,EDNRB,ADRA2B,GDF10,COLEC11,CXCL12,RAMP1,ITGB3,HGF,NTF3
positive regulation of leukocyte migration	GO:0002687	0.025731626	1.589532774	148	45	5	21257	PTAFR,PLVAP,DOCK8,CXCL12,ITGB3
response to organic substance	GO:0010033	0.027374417	1.562655126	3351	48	20	21257	HHIP,BMP10,NRXN1,GDF2,PTAFR,NR1H5,PDE8B,LRAT,EDNRB,PLVAP,ALPL, DOCK8,GDF10,ADAMTS13,ITIH4,CXCL12,RAMP1,ITGB3,HGF,NTF3
regulation of cellular component movement	GO:0051270	0.031157411	1.506438634	1057	48	11	21257	BMP10,GDF2,PTAFR,RELN,PLVAP,NTN1,DOCK8,CXCL12,ITGB3,HGF,NTF3
positive chemotaxis	GO:0050918	0.03430169	1.464684481	71	48	4	21257	COLEC10,CXCL12,HGF,NTF3
response to pain	GO:0048265	0.036880101	1.433207897	36	32	3	21257	RELN,EDNRB,GJA4
system development	GO:0048731	0.039461172	1.403830023	4738	48	24	21257	HHIP,BMP10,NRXN1,GDF2,ANGPTL6,RELN,NTM,C6,RSPO3,DCDC2A,EDNRB, CLSTN3,SLCO2B1,ADRA2B,ALPL,GJA4,NTN1,MUSTN1,CXCL12,ANK3,RAMP1,ITGB3, HGF,NTF3
heterophilic cell-cell adhesion via plasma membrane cell adhesion molecules	GO:0007157	0.043203205	1.36448403	44	4	2	21257	COLEC10,NRXN1
response to external stimulus	GO:0009605	0.043539509	1.361116478	2857	48	18	21257	COLEC10,NRXN1,FCNA,PTAFR,RELN,NR1H5,SUCNR1,LRAT,EDNRB,ALPL,NTN1, ADAMTS13,COLEC11,CXCL12,ANK3,ITGB3,HGF,NTF3
regulation of synapse maturation	GO:0090128	0.043911322	1.357423489	15	11	2	21257	NRXN1,RELN
positive regulation of cell differentiation	GO:0045597	0.04397047	1.356838889	1097	48	11	21257	BMP10,GDF2,RELN,ADRA2B,NTN1,GDF10,MUSTN1,CXCL12,ITGB3,HGF,NTF3
anatomical structure development	GO:0048856	0.047751098	1.321016642	5869	48	27	21257	HHIP,COLEC10,BMP10,NRXN1,GDF2,ANGPTL6,RELN,NR1H5,SHISA3,NTM,C6,RSPO3, DCDC2A,EDNRB,CLSTN3,SLCO2B1,ADRA2B,ALPL,GJA4,NTN1,MUSTN1,CXCL12, ANK3,RAMP1,ITGB3,HGF,NTF3
learning	GO:0007612	0.049927996	1.301655862	167	23	4	21257	NRXN1,RELN,PDE8B,DCDC2A
cell surface	GO:0009986	5.47E-06	5.262233381	1062	45	14	21187	HHIP,BMP10,NRXN1,FCNA,NTM,SUCNR1,CLSTN3,PLVAP,SLCO2B1,ADRA2B, CXCL12,ANK3,RAMP1,ITGB3
extracellular region	GO:0005576	2.80E-05	4.55272153	2713	48	21	21187	HHIP,COLEC10,BMP10,FCNA,GDF2,ANGPTL6,RELN,NTM,C6,RSPO3,ALPL,NTN1, GDF10,ADAMTS13,ITIH4,SOD3,COLEC11,CXCL12,RAMP1,HGF,NTF3
extracellular space	GO:0005615	0.002563378	2.591187325	1885	48	15	21187	COLEC10,BMP10,GDF2,RELN,NTM,C6,ALPL,GDF10,ADAMTS13,SOD3,COLEC11, CXCL12,RAMP1,HGF,NTF3
cell periphery	GO:0071944	0.041321731	1.383821494	6375	46	26	21187	HHIP,NRXN1,VIPR1,FCNA,PTAFR,RELN,NTM,SUCNR1,C6,DCDC2A,EDNRB,STEAP4, CLSTN3,PLVAP,SLCO2B1,ADRA2B,ALPL,GJA4,NTN1,DOCK8,ITIH4,CXCL12,ANK3,RAMP1,ITGB3,CADM3
Lectin pathway of complement activation	AC:R-MMU-166	0.002001741	2.698592149	7	6	2	8671	COLEC10,FCNA

Table S5 (Related to Figures 4, S4). Functional enrichment analysis in mouse myCAF common to YAP/AKT- and KRAS/p19-induced ICC models performed using g:Profiler.

term_name	term id	adjusted p value	negative log10 of adjusted p value	term size	query size	intersection size	effective domain size	intersections
enzyme inhibitor activity	GO:0004857	3.47E-05	4.4598658	385	22	7	21095	LEF1,PTN,ITIH5,CDKN2A,SERPINF1,CDKN2B,COL7A1
extracellular matrix structural constituent	GO:0005201	9.07E-05	4.0423069	128	43	6	21095	COL15A1,COL8A1,FBN2,COL7A1,MFAP4,PCOLCE2
molecular function regulator	GO:0098772	0.000967479	3.0143584	1799	13	8	21095	DKK2,LEF1,LRRC55,PTN,CRLF1,ITIH5,CDKN2A,SERPINF1
extracellular matrix structural constituent conferring tensile strength	GO:0030020	0.002326147	2.6333629	34	22	3	21095	COL15A1,COL8A1,COL7A1
enzyme regulator activity	GO:0030234	0.00600966	2.2211501	974	26	8	21095	LEF1,PTN,ITIH5,CDKN2A,SERPINF1,CDKN2B,COL7A1,WNT11
frizzled binding	GO:0005109	0.00692556	2.1595451	41	26	3	21095	ROR2,SFRP1,WNT11
cyclin-dependent protein serine/threonine kinase inhibitor activity	GO:0004861	0.01619062	1.7907365	12	17	2	21095	CDKN2A,CDKN2B
endopeptidase inhibitor activity	GO:0004866	0.019073091	1.7195789	197	22	4	21095	LEF1,ITIH5,SERPINF1,COL7A1
palmitoleyl hydrolase activity	GO:1990699	0.019114757	1.7186312	1	1	1	21095	NOTUM
endopeptidase regulator activity	GO:0061135	0.024007277	1.6196571	209	22	4	21095	LEF1,ITIH5,SERPINF1,COL7A1
peptidase inhibitor activity	GO:0030414	0.024912229	1.6035874	211	22	4	21095	LEF1,ITIH5,SERPINF1,COL7A1
peptidase regulator activity	GO:0061134	0.046553337	1.3320492	248	22	4	21095	LEF1,ITIH5,SERPINF1,COL7A1
animal organ morphogenesis	GO:0009887	3.79E-07	6.4214431	1028	34	14	21257	LEF1,PTN,HAS2,CDKN2A,COL8A1,FBN2,ROR2,COL7A1,ETV4,SFRP1,WNT11,ACTG2,TMEFF1,FST
tissue development	GO:0009888	1.70E-06	5.7683194	1923	34	17	21257	LEF1,PTN,HAS2,CRLF1,MEOX1,CDKN2A,MEGF10,COL8A1,FBN2,ROR2,COL7A1,ETV4,SFRP1,WNT11,ACTG2,TMEFF1,FST
negative regulation of canonical Wnt signaling pathway	GO:0090090	1.87E-05	4.7292438	130	26	6	21257	NOTUM,DKK2,NKD2,ROR2,SFRP1,WNT11
negative regulation of epithelial cell proliferation	GO:0050680	1.98E-05	4.704054	137	25	6	21257	PTN,CDKN2A,SERPINF1,CDKN2B,ETV4,SFRP1
epithelial cell proliferation	GO:0050673	2.74E-05	4.5616184	420	34	9	21257	PTN,HAS2,CDKN2A,SERPINF1,COL8A1,CDKN2B,ETV4,SFRP1,FST
negative regulation of Wnt signaling pathway	GO:0030178	5.56E-05	4.2547247	156	26	6	21257	NOTUM,DKK2,NKD2,ROR2,SFRP1,WNT11
canonical Wnt signaling pathway	GO:0060070	7.01E-05	4.1541574	283	26	7	21257	NOTUM,DKK2,LEF1,NKD2,ROR2,SFRP1,WNT11
regulation of Wnt signaling pathway	GO:0030111	9.76E-05	4.0106231	297	26	7	21257	NOTUM,DKK2,LEF1,NKD2,ROR2,SFRP1,WNT11
somite development	GO:0061053	0.00015159	3.819329	91	26	5	21257	LEF1,MEOX1,ROR2,SFRP1,WNT11
regulation of epithelial cell proliferation	GO:0050678	0.000239095	3.6214299	354	25	7	21257	PTN,HAS2,CDKN2A,SERPINF1,CDKN2B,ETV4,SFRP1
anatomical structure morphogenesis	GO:0009653	0.000250836	3.6006109	2673	34	17	21257	LEF1,PTN,HAS2,MEOX1,CDKN2A,SERPINF1,COL8A1,FBN2,ROR2,COL7A1,ETV4,SFRP1,WNT11,ACTG2,TMEFF1,CSPG4,FST
multicellular organism development	GO:0007275	0.000349921	3.4560297	5293	34	23	21257	DKK2,LEF1,PTN,HAS2,CRLF1,MEOX1,CDKN2A,MEGF10,SERPINF1,AMN,COL8A1,CDKN2B,FBN2,ROR2,COL7A1,GFRA2,ETV4,SFRP1,WNT11,ACTG2,TMEFF1,CSPG4,FST
cell population proliferation	GO:0008283	0.00036649	3.4359376	2065	34	15	21257	LEF1,PTN,HAS2,CRLF1,CDKN2A,MEGF10,SERPINF1,COL8A1,CDKN2B,ROR2,ETV4,SFRP1,WNT11,CSPG4,FST
animal organ development	GO:0048513	0.000368885	3.4331091	3508	34	19	21257	LEF1,PTN,HAS2,CRLF1,MEOX1,CDKN2A,MEGF10,SERPINF1,COL8A1,CDKN2B,FBN2,ROR2,COL7A1,ETV4,SFRP1,WNT11,ACTG2,TMEFF1,FST
regulation of cell population proliferation	GO:0042127	0.00054261	3.2655122	1739	26	12	21257	LEF1,PTN,HAS2,CRLF1,CDKN2A,MEGF10,SERPINF1,CDKN2B,ROR2,ETV4,SFRP1,WNT11
regulation of canonical Wnt signaling pathway	GO:0060828	0.000646058	3.1897284	236	26	6	21257	NOTUM,DKK2,NKD2,ROR2,SFRP1,WNT11
Wnt signaling pathway	GO:0016055	0.000814126	3.0893082	406	26	7	21257	NOTUM,DKK2,LEF1,NKD2,ROR2,SFRP1,WNT11
cell-cell signaling by wnt	GO:0198738	0.0008415	3.0749458	408	26	7	21257	NOTUM,DKK2,LEF1,NKD2,ROR2,SFRP1,WNT11
system development	GO:0048731	0.001607888	2.7937443	4738	34	21	21257	LEF1,PTN,HAS2,CRLF1,MEOX1,CDKN2A,MEGF10,SERPINF1,COL8A1,CDKN2B,FBN2,ROR2,COL7A1,GFRA2,ETV4,SFRP1,WNT11,ACTG2,TMEFF1,CSPG4,FST
negative regulation of cell population proliferation	GO:0008285	0.002140547	2.6694752	691	26	8	21257	PTN,CDKN2A,SERPINF1,CDKN2B,ROR2,ETV4,SFRP1,WNT11
cellular response to growth factor stimulus	GO:0071363	0.002489148	2.6039494	651	37	9	21257	LEF1,PTN,HAS2,CDKN2B,FBN2,ROR2,SFRP1,FST,NREP
anatomical structure development	GO:0048856	0.002590896	2.5865499	5869	34	23	21257	DKK2,LEF1,PTN,HAS2,CRLF1,MEOX1,CDKN2A,MEGF10,SERPINF1,AMN,COL8A1,CDKN2B,FBN2,ROR2,COL7A1,GFRA2,ETV4,SFRP1,WNT11,ACTG2,TMEFF1,CSPG4,FST
apoptotic process involved in development	GO:1902742	0.002595238	2.5858229	44	11	3	21257	LEF1,CDKN2A,MEGF10
transmembrane receptor protein serine/threonine kinase signaling pathway	GO:0007178	0.002761108	2.5589165	331	37	7	21257	LEF1,CDKN2B,FBN2,ROR2,SFRP1,FST,NREP
somitogenesis	GO:0001756	0.00278857	2.5546185	72	25	4	21257	LEF1,MEOX1,ROR2,SFRP1
response to growth factor	GO:0070848	0.003480667	2.4583375	678	37	9	21257	LEF1,PTN,HAS2,CDKN2B,FBN2,ROR2,SFRP1,FST,NREP
gland development	GO:0048732	0.003595869	2.4441962	507	26	7	21257	LEF1,PTN,CDKN2A,SERPINF1,ETV4,SFRP1,WNT11
mesenchyme development	GO:0060485	0.003700311	2.4317618	263	31	6	21257	LEF1,HAS2,MEOX1,SFRP1,WNT11,ACTG2
cell surface receptor signaling pathway involved in cell-cell signaling	GO:1905114	0.004253448	2.3712588	520	26	7	21257	NOTUM,DKK2,LEF1,NKD2,ROR2,SFRP1,WNT11
regulation of cell differentiation	GO:0045595	0.004395212	2.3570202	1950	37	14	21257	LEF1,PTN,HAS2,CDKN2A,MEGF10,SERPINF1,CDKN2B,FBN2,ROR2,SFRP1,WNT11,CSPG4,FST,NREP
negative regulation of cellular protein metabolic process	GO:0032269	0.00459014	2.3381741	1095	25	9	21257	LEF1,PTN,ITIH5,CDKN2A,SERPINF1,CDKN2B,COL7A1,GFRA2,SFRP1
negative regulation of catalytic activity	GO:0043086	0.005250512	2.2797983	815	25	8	21257	LEF1,PTN,ITIH5,CDKN2A,SERPINF1,CDKN2B,COL7A1,SFRP1
developmental process	GO:0032502	0.005622236	2.250091	6410	37	25	21257	DKK2,LEF1,PTN,HAS2,CRLF1,MEOX1,CDKN2A,MEGF10,SERPINF1,AMN,COL8A1,CDKN2B,FBN2,ROR2,COL7A1,GFRA2,ETV4,SFRP1,WNT11,ACTG2,TMEFF1,CSPG4,FST,B4GALNT1,NREP
regulation of animal organ morphogenesis	GO:2000027	0.006346416	2.1974714	193	26	5	21257	PTN,CDKN2A,ROR2,SFRP1,WNT11
negative regulation of protein metabolic process	GO:0051248	0.007276934	2.1380516	1158	25	9	21257	LEF1,PTN,ITIH5,CDKN2A,SERPINF1,CDKN2B,COL7A1,GFRA2,SFRP1
tube development	GO:0035295	0.007436059	2.1286572	1109	26	9	21257	LEF1,PTN,HAS2,CRLF1,SERPINF1,COL8A1,ETV4,SFRP1,WNT11
negative regulation of molecular function	GO:0044092	0.007485931	2.1257542	1162	25	9	21257	DKK2,LEF1,PTN,ITIH5,CDKN2A,SERPINF1,CDKN2B,COL7A1,SFRP1
regulation of cellular protein metabolic process	GO:0032268	0.008003309	2.0967304	2681	26	13	21257	LEF1,PTN,CRLF1,ITIH5,CDKN2A,SERPINF1,NKD2,CDKN2B,ROR2,COL7A1,GFRA2,SFRP1,WNT11
epithelium development	GO:0060429	0.008362337	2.0776723	1125	26	9	21257	LEF1,PTN,CRLF1,MEOX1,CDKN2A,ROR2,ETV4,SFRP1,WNT11
regulation of cell adhesion	GO:0030155	0.008503341	2.0704104	689	15	6	21257	LEF1,PTN,HAS2,CDKN2A,MEGF10,COL8A1
segmentation	GO:0035282	0.009591856	2.0180973	98	25	4	21257	LEF1,MEOX1,ROR2,SFRP1
anatomical structure formation involved in morphogenesis	GO:0048646	0.00986788	2.0057761	1148	26	9	21257	LEF1,PTN,MEOX1,SERPINF1,COL8A1,FBN2,ROR2,SFRP1,WNT11
negative regulation of cellular process	GO:0048523	0.009918832	2.0035395	4911	26	17	21257	NOTUM,DKK2,LEF1,PTN,CRLF1,ITIH5,CDKN2A,SERPINF1,NKD2,CDKN2B,FBN2,ROR2,COL7A1,GFRA2,ETV4,SFRP1,WNT11
ossification	GO:0001503	0.010108895	1.9952963	379	26	6	21257	LEF1,PTN,FBN2,ROR2,SFRP1,WNT11
tube morphogenesis	GO:0035239	0.011575283	1.9364684	892	33	9	21257	LEF1,PTN,HAS2,SERPINF1,COL8A1,ETV4,SFRP1,WNT11,CSPG4
tissue morphogenesis	GO:0048729	0.011814853	1.9275717	644	34	8	21257	LEF1,ROR2,COL7A1,ETV4,SFRP1,WNT11,ACTG2,FST
positive regulation of cell adhesion	GO:0045785	0.012526189	1.902181	408	15	5	21257	LEF1,PTN,HAS2,MEGF10,COL8A1
negative regulation of developmental process	GO:0051093	0.013121531	1.8820155	1126	34	10	21257	LEF1,PTN,CDKN2A,SERPINF1,CDKN2B,ETV4,SFRP1,WNT11,CSPG4,FST
regulation of multicellular organismal development	GO:2000026	0.014058579	1.8520586	2152	37	14	21257	LEF1,PTN,CDKN2A,MEGF10,SERPINF1,CDKN2B,FBN2,ROR2,ETV4,SFRP1,WNT11,CSPG4,FST,NREP
regulation of protein metabolic process	GO:0051246	0.016828218	1.7739619	2864	26	13	21257	LEF1,PTN,CRLF1,ITIH5,CDKN2A,SERPINF1,NKD2,CDKN2B,ROR2,COL7A1,GFRA2,SFRP1,WNT11
skeletal system morphogenesis	GO:0048705	0.01752666	1.7563008	248	25	5	21257	HAS2,FBN2,ROR2,COL7A1,SFRP1
cell adhesion	GO:0007155	0.018468995	1.7335567	1298	25	9	21257	LEF1,PTN,HAS2,CDKN2A,MEGF10,COL15A1,COL8A1,COL7A1,SFRP1
biological adhesion	GO:0022610	0.019775926	1.7038632	1309	25	9	21257	LEF1,PTN,HAS2,CDKN2A,MEGF10,COL15A1,COL8A1,COL7A1,SFRP1
sensory organ development	GO:0007423	0.020997299	1.6778366	577	20	6	21257	LEF1,PTN,SERPINF1,COL8A1,FBN2,ROR2
bone mineralization	GO:0030282	0.022058952	1.6564151	116	26	4	21257	PTN,FBN2,ROR2,WNT11
regulation of cell-substrate adhesion	GO:0010810	0.022732149	1.6433595	211	15	4	21257	PTN,HAS2,CDKN2A,COL8A1
skeletal system development	GO:0001501	0.025571105	1.5922505	509	34	7	21257	HAS2,FBN2,ROR2,COL7A1,SFRP1,WNT11,FST
Wnt signaling pathway, planar cell polarity pathway	GO:0060071	0.025613855	1.5915251	38	26	3	21257	ROR2,SFRP1,WNT11
planar cell polarity pathway involved in axis elongation	GO:0003402	0.02760231	1.5590546	5	26	2	21257	SFRP1,WNT11
estrous cycle	GO:0044849	0.029420928	1.5313436	22	6	2	21257	PTN,HAS2
enzyme linked receptor protein signaling pathway	GO:0007167	0.029884227	1.524558	884	37	9	21257	LEF1,CDKN2B,FBN2,ROR2,GFRA2,SFRP1,CSPG4,FST,NREP
regulation of establishment of planar polarity	GO:0090175	0.029949564	1.5236095	40	26	3	21257	ROR2,SFRP1,WNT11
cell surface receptor signaling pathway	GO:0007166	0.032521937	1.4878236	2655	37	15	21257	NOTUM,DKK2,LEF1,PTN,CRLF1,NKD2,CDKN2B,FBN2,ROR2,GFRA2,SFRP1,WNT11,CSPG4,FST,NREP
ovulation cycle	GO:0042698	0.034149574	1.4666147	86	13	3	21257	PTN,HAS2,SERPINF1
negative regulation of mammary gland epithelial cell proliferation	GO:0033600	0.035143454	1.4541556	6	24	2	21257	CDKN2A,ETV4

cell differentiation	GO:0030154	0.038207701	1.4178491	4248	34	18	21257	LEF1,PTN,HAS2,MEOX1,CDKN2A,MEGF10,SERPINF1,COL8A1,CDKN2B,FBN2,ROR2,COL7A1,ETV4,SFRP1,WNT11,TMEFF1,CSPG4,FST
gland morphogenesis	GO:0022612	0.038280124	1.4170267	139	25	4	21257	PTN,CDKN2A,ETV4,SFRP1
negative regulation of multicellular organismal process	GO:0051241	0.040857245	1.3887309	1326	33	10	21257	LEF1,PTN,CDKN2A,SERPINF1,CDKN2B,ETV4,SFRP1,WNT11,ADCY7,CSPG4
epithelial to mesenchymal transition	GO:0001837	0.042519125	1.3714157	137	26	4	21257	LEF1,HAS2,SFRP1,WNT11
negative regulation of biological process	GO:0048519	0.047486952	1.3234257	5477	26	17	21257	NOTUM,DKK2,LEF1,PTN,CRLF1,ITIH5,CDKN2A,SERPINF1,NKD2,CDKN2B,FBN2,ROR2,COL7A1,GFRA2,ETV4,SFRP1,WNT11
cellular response to platelet-derived growth factor stimulus	GO:0036120	0.048107092	1.3177909	28	6	2	21257	PTN,HAS2
collagen-containing extracellular matrix	GO:0062023	1.87E-11	10.727259	339	43	13	21187	PTN,ITIH5,COL15A1,SERPINF1,COL8A1,FBN2,COL7A1,SFRP1,TMEFF1,CSPG4,S100A6,MFAP4,PCOLCE2
extracellular matrix	GO:0031012	3.25E-11	10.487735	452	43	14	21187	PTN,ITIH5,COL15A1,SERPINF1,COL8A1,FBN2,COL7A1,SFRP1,WNT11,TMEFF1,CSPG4,S100A6,MFAP4,PCOLCE2
extracellular region	GO:0005576	5.76E-07	6.2396066	2713	44	22	21187	NOTUM,DKK2,PTN,CRLF1,ITIH5,COL15A1,SERPINF1,AMN,COL8A1,FBN2,COL7A1,SFRP1,WNT11,PRSS35,TMEFF1,CSPG4,FST,S100A6,PLA1A,MFAP4,PCOLCE2,TNFRSF9
basement membrane	GO:0005604	2.18E-06	5.6623636	104	32	6	21187	PTN,COL15A1,SERPINF1,COL8A1,COL7A1,TMEFF1
extracellular space	GO:0005615	0.003622364	2.4410079	1885	44	14	21187	DKK2,PTN,CRLF1,COL15A1,SERPINF1,AMN,COL8A1,COL7A1,SFRP1,WNT11,FST,PLA1A,MFAP4,TNFRSF9
collagen trimer	GO:0005581	0.022181242	1.6540141	88	22	3	21187	COL15A1,COL8A1,COL7A1
microfibril	GO:0001527	0.039580835	1.4025151	11	39	2	21187	FBN2,MFAP4
Wnt signaling pathway	KEGG:04310	5.64E-05	4.248439	152	26	7	6926	NOTUM,DKK2,LEF1,NKD2,ROR2,SFRP1,WNT11
Cushing syndrome	KEGG:04934	0.017493086	1.7571336	146	29	5	6926	LEF1,CDKN2A,CDKN2B,WNT11,ADCY7
Collagen chain trimerization	AC:R-MMU-8948	0.026137604	1.5827342	38	22	3	8671	COL15A1,COL8A1,COL7A1
Collagen biosynthesis and modifying enzymes	AC:R-MMU-1650	0.045313253	1.3437748	59	43	4	8671	COL15A1,COL8A1,COL7A1,PCOLCE2
Factor: AP-2; motif: SNNNCCNCAGGCN; match class: 1	TF:M00915_1	0.010591738	1.9750328	2395	48	17	21846	NOTUM,LEF1,LRRC55,CRLF1,SERPINF1,NKD2,CDKN2B,FBN2,ROR2,ADCY7,ACTG2,TMEFF1,FST,MFAP4,VCAN,CPXM2,DOK5
Factor: Smad4; motif: NCAGACAN; match class: 0	TF:M07368_0	0.010657189	1.9723573	5290	40	23	21846	DKK2,LRRC55,HAS2,CRLF1,MEOX1,CDKN2A,MEGF10,SERPINF1,COL8A1,NKD2,COL7A1,ETV4,SFRP1,WNT11,D630003M21RIK,PRSS35,ADCY7,ACTG2,TMEFF1,CSPG4,S100A6,MFAP4,LSP1
Factor: Smad4; motif: NCAGACAN	TF:M07368	0.010657189	1.9723573	5290	40	23	21846	DKK2,LRRC55,HAS2,CRLF1,MEOX1,CDKN2A,MEGF10,SERPINF1,COL8A1,NKD2,COL7A1,ETV4,SFRP1,WNT11,D630003M21RIK,PRSS35,ADCY7,ACTG2,TMEFF1,CSPG4,S100A6,MFAP4,LSP1
Factor: Sp3; motif: ASMCTTGGGSRGGG; match class: 1	TF:M00665_1	0.018213747	1.7396007	1757	41	13	21846	LEF1,CRLF1,MEOX1,MEGF10,FBN2,INSC,COL7A1,ETV4,WNT11,CSPG4,FST,NREP,VCAN
Factor: FKLF; motif: BGGGNGGVMD; match class: 1	TF:M01837_1	0.026764655	1.5724384	985	27	8	21846	DKK2,LEF1,HAS2,NKD2,ROR2,GFRA2,ETV4,D630003M21RIK
Factor: WT1; motif: SMCNCCNSC	TF:M01118	0.032278059	1.4910926	8133	27	21	21846	NOTUM,DKK2,LEF1,HAS2,CRLF1,MEOX1,ITIH5,CDKN2A,MEGF10,AMN,NKD2,CDKN2B,FBN2,INSC,ROR2,COL7A1,GFRA2,ETV4,SFRP1,WNT11,D630003M21RIK
Factor: WT1; motif: SMCNCCNSC; match class: 0	TF:M01118_0	0.032278059	1.4910926	8133	27	21	21846	NOTUM,DKK2,LEF1,HAS2,CRLF1,MEOX1,ITIH5,CDKN2A,MEGF10,AMN,NKD2,CDKN2B,FBN2,INSC,ROR2,COL7A1,GFRA2,ETV4,SFRP1,WNT11,D630003M21RIK

Table S6 (Related to Figure 6). Combined top DGE core matrisome filtered CAF YAP/AKT and KRAS/p19 versus quiescent HSC.

Gene	baseMean	log2FoldChange YAP/AKT	lfcSE	stat	pvalue	padj	baseMean	log2FoldChange KRAS/p19	lfcSE	stat	pvalue	padj	Sum log2Fold Kras/p19 and YAP/AKT	
Mgp	9960.9976	13.3806	0.6823	-19.6120	1.22E-85	1.11E-82	4142.7631	12.1766	0.5451	-22.3367	1.63E-110	1.36E-107	25.5572	Core Matrisome
Col6a5	2969.9244	13.1437	1.1259	-11.6744	1.72E-31	1.79E-29	967.4053	11.6372	0.9047	-12.8630	7.27E-38	6.65E-36	24.7809	Core Matrisome
Spp1	15673.0196	12.0905	0.5016	-24.1062	2.15E-128	9.40E-125	15253.7126	12.1529	0.4242	-28.6461	1.79E-180	4.34E-177	24.2434	Core Matrisome
Col6a6	963.6615	12.6791	1.3962	-9.0814	1.07E-19	4.95E-18	231.4441	10.6974	1.6731	-6.3936	1.62E-10	2.27E-09	23.3765	Core Matrisome
Col15a1	15353.4502	11.2533	0.8004	-14.0593	6.76E-45	1.45E-42	12457.9640	11.1875	0.8002	-13.9810	2.04E-44	2.28E-42	22.4408	Core Matrisome
Mfap4	2391.5150	11.4487	1.1358	-10.0801	6.76E-24	4.32E-22	1234.1193	10.5493	1.2482	-8.4515	2.88E-17	7.83E-16	21.9980	Core Matrisome
Fbn2	9533.2964	11.5753	0.4199	-27.5667	2.79E-167	2.03E-163	1643.1586	9.1123	0.3408	-26.7375	1.72E-157	3.76E-154	20.6877	Core Matrisome
Cilp	1370.9420	10.3084	1.0201	-10.1053	5.23E-24	3.39E-22	1237.1727	10.2419	0.8896	-11.5124	1.14E-30	7.41E-29	20.5503	Core Matrisome
Dmbt1	289.6714	11.0294	2.0308	-5.4310	5.60E-08	6.41E-07	94.1498	9.4647	1.1964	-7.9113	2.55E-15	5.89E-14	20.4941	Core Matrisome
Igfbp5	5785.2698	10.7093	0.4993	-21.4477	4.79E-102	1.16E-98	2744.1844	9.7364	0.3274	-29.7352	2.70E-194	7.34E-191	20.4457	Core Matrisome
Lamc3	434.4838	10.7764	1.4269	-7.5524	4.27E-14	1.14E-12	176.7730	9.5884	1.0171	-9.4270	4.22E-21	1.47E-19	20.3648	Core Matrisome
Has2	**240.0764**	**10.0202**	**1.0867**	**-9.2209**	**2.95E-20**	**1.44E-18**	**266.4770**	**10.2429**	**1.0519**	**-9.7375**	**2.09E-22**	**8.13E-21**	**20.2631**	**Core Matrisome**
Igfbp6	243.2684	10.0338	1.1285	-8.8914	6.03E-19	2.58E-17	250.1232	10.1387	1.0424	-9.7263	2.33E-22	9.04E-21	20.1726	Core Matrisome
Col10a1	48.5075	9.1512	1.1911	-7.6831	1.55E-14	4.41E-13	91.6773	10.1460	1.0657	-9.5208	1.72E-21	6.18E-20	19.2973	Core Matrisome
Col28a1	67.8336	9.6355	1.1450	-8.4152	3.92E-17	1.43E-15	62.1539	9.5822	1.1508	-8.3268	8.31E-17	2.20E-15	19.2177	Core Matrisome
Npnt	33.5049	8.6128	1.1403	-7.5534	4.24E-14	1.13E-12	58.0432	9.4710	1.1570	-8.1861	2.70E-16	6.80E-15	18.0838	Core Matrisome
Thbs4	327.9637	9.2556	1.2470	-7.4220	1.15E-13	2.93E-12	197.6863	8.5902	1.3166	-6.5247	6.82E-11	9.90E-10	17.8458	Core Matrisome
Smoc1	231.6377	8.6320	0.8131	-10.6162	2.50E-26	1.87E-24	147.9011	8.0631	0.6929	-11.6363	2.69E-31	1.83E-29	16.6951	Core Matrisome
Mfap5	41.7127	6.7429	1.0069	-6.6968	2.13E-11	4.14E-10	332.4165	9.7752	0.8407	-11.6270	3.00E-31	2.03E-29	16.5181	Core Matrisome